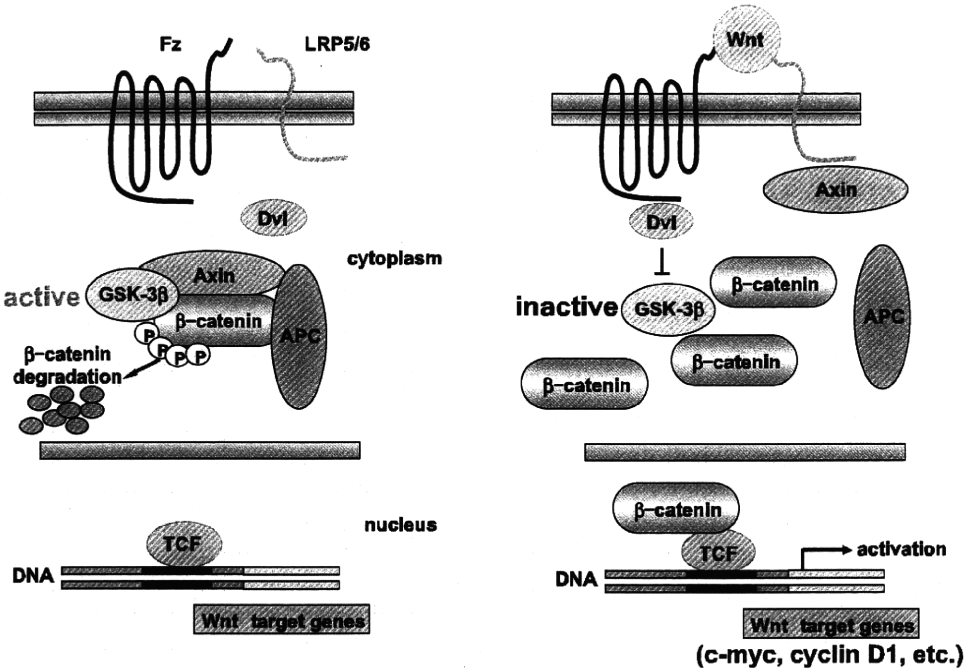


**Fig. 1.** The Wnt/$\beta$-catenin signaling pathway. In the absence of Wnt, $\beta$-catenin binds to the protein complex formed by axin, APC, and GSK-3$\beta$ and then is phosphorylated by GSK-3$\beta$, resulting in its degradation by the 26S proteasome system (left). Wnt binds to the receptor Fz and the co-receptor LRP5/6, and these receptors mediate signal transduction in cells. GSK-3$\beta$ and CK1$\alpha$ are inhibited by activated Dvl; thus $\beta$-catenin escapes phosphorylation. Unphosphorylated $\beta$-catenin accumulates in the cytoplasm and translocates to the nucleus. In the nucleus, $\beta$-catenin activates the transcription of target genes together with TCF (right). Fz, Frizzled; LRP, low-density lipoprotein receptor–related protein; Dvl, disheveled; APC, adenomatous polyposis coli; GSK-3$\beta$, glycogen synthase kinase-3$\beta$; TCF, T-cell factor.

proteasome complex (10, 11). After the Wnt proteins bind to the receptor complex Frizzleds/low-density lipoprotein receptor–related protein (Fz/LRP), cytoplasmic disheveled (Dvl), a protein downstream of the receptor complex, is phosphorylated and inhibits GSK-3$\beta$ by causing their retention at the scaffolding protein axin, resulting in the accumulation of non-phosphorylated $\beta$-catenin in the cytoplasm. Non-phosphorylated $\beta$-catenin avoids degradation and translocates into the nucleus. In the nucleus, $\beta$-catenin forms a complex with the transcription factor TCF and induces the transcription of downstream target genes (1 – 3). Thus GSK-3$\beta$ plays a critical role in the regulation of Wnt/$\beta$-catenin target gene expression by controlling the level of cytoplasmic $\beta$-catenin (Fig. 1).

## Cyclin D1 and GSK-3$\beta$

Since several oncogenes are included amongst the target genes, constitutive activation of the Wnt/$\beta$-catenin signaling pathway can lead to cancer (12). One oncogene, the cyclin D1 gene CCND1, is a well-known Wnt/$\beta$-catenin target gene.

The cell cycle progresses through four sequential phases, namely, gap 1 (G1), synthesis (S), gap 2 (G2), and mitosis (M) phases. Passage through the cell cycle is strictly controlled by cyclin/cyclin-dependent kinase (CDK) complexes. During the G1 phase, cells need to decide whether to advance towards another division or withdraw from the cell cycle into the quiescence phase (G0) in response to extracellular signals. The point at which this decision is made is called the restriction point. Cyclin D (D1, D2, and D3) act as a mitogenic signal sensor and is expressed as a delayed early response to many mitogenic signals, which forces cells to enter the proliferative cycle from the G0 phase (13, 14). The cyclin D mRNA level is dramatically increased following mitogenic stimulation, and both mRNA and protein levels of cyclin D1 are strictly regulated after induction. Cyclin D forms a complex with and functions as a regulatory subunit of CDK4 or 6, the activity of which is required for the transition from the G1 phase to the S phase (Fig. 2).

In tumor cells, genes encoding the proteins that directly regulate the cell cycle are often quantitatively altered. Among these proteins, cyclin D1 is strongly

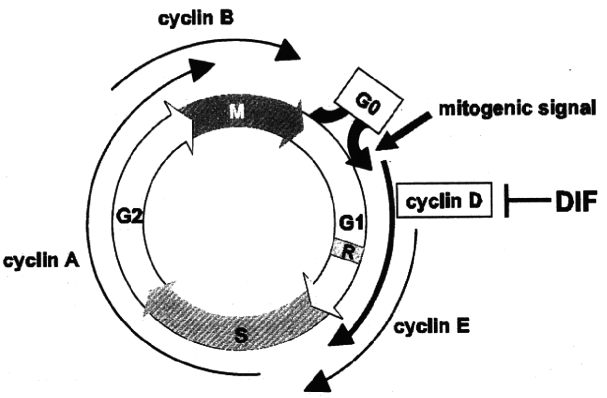


**Fig. 2.** Schematic representation of the mammalian cell cycle and its regulatory molecules. The cell cycle progresses through four sequential phases, gap 1 (G1), synthesis (S), gap 2 (G2), and mitosis (M) phases. Passage through the cell cycle is controlled by cyclin /cyclin-dependent kinase complexes and each cyclin exhibits a characteristic pattern of expression and degradation. Among cyclins, cyclin D acts as a mitogenic signal sensor and is expressed as an early response to many mitogenic signals, which forces cells to enter the proliferative cycle from the G0 phase. DIFs inhibit mammalian cell proliferation by suppressing the expression of cyclin D1 mRNA and protein. R, restriction point.

implicated in oncogenesis (14). Amplification of the gene encoding cyclin D1 and overexpression of cyclin D1 protein are often found in several types of human malignant neoplasms (15 – 18). Thus cyclin D1 is particularly well known for its prominent role in driving tumorigenesis. Other members of the cyclin D family, cyclins D2 and D3, are also expressed in an overlapping and redundant fashion with cyclin D1 in all proliferating cell types and are overexpressed in human cancers, but much less commonly than cyclin D1 (19).

The level of the cyclin D1 protein is regulated by an ubiquitin-dependent mechanism throughout the progression of the cell cycle. Cyclin D1 is transported from the nucleus to the cytoplasm where it is degraded by the 26S proteasome. Although GSK-3$\beta$ is a cytosolic protein, it is translocated into the nucleus when activated and phosphorylates cyclin D1 on $Thr^{286}$, thereby stimulating cyclin D1 turnover in response to mitogenic signals (7, 20, 21). Phosphorylation of cyclin D1 on $Thr^{286}$ by GSK-3$\beta$ facilitates its association with CRM1, which is a nuclear protein that mediates the nuclear export of proteins, resulting in the exclusion of cyclin D1 from the nucleus to initiate its proteasomal degradation (22).

As described above, cyclin D1 gene expression is activated by Wnt/$\beta$-catenin signaling, in which GSK-3$\beta$ plays a critical role in its regulation, and cyclin D1 protein degradation is regulated by GSK-3$\beta$. Thus activation of GSK-3$\beta$ is expected to lead to a reduction in the level of cyclin D1 mRNA at the transcriptional level and the protein at the degradation level. While many diseases, including diabetes mellitus and Alzheimer's disease, can be ameliorated by the use of GSK-3$\beta$ inhibitors, cancers, especially cancers in which cyclin D1 is overexpressed, are likely to be more susceptible to pharmacological activation of GSK-3$\beta$.

## Differentiation-inducing factors: modulators of the Wnt/$\beta$-catenin signaling pathway and potent anti-tumor agents

Differentiation-inducing factors (DIFs) were identified in *Dictyostelium discoideum* as the morphogens required for stalk cell differentiation (23). In the DIF family, DIF-1 [1-(3,5-dichloro-2,6-dihydroxy-4-methoxyphenyl)-1-hexanone] was the first to be identified and DIF-3, the monochlorinated analog of DIF-1, is a natural metabolite of DIF-1 in *Dictyostelium* (24). However, the actions of DIFs are not limited to *Dictyostelium*. They also have strong effects on mammalian cells. DIF-1 and/or DIF-3 strongly inhibit proliferation and induce differentiation in several leukemia cells, including the murine erythroleukemia cell line B8, human leukemia cell line K562, and human myeloid leukemia cell line HL-60 (25, 26). DIF-3 has been reported to have the most potent antiproliferative effect on mammalian leukemia cells among the DIF analog examined to date (27).

However, the target molecule (receptor) of DIFs is unknown and it is not clear even in *Dictyostelium* how DIFs induce antiproliferative effects and cell differentiation. DIFs are small hydrophobic molecules and are therefore expected to be able to cross cell membranes without requiring channels or carriers. In search of chemical substances applicable for the treatment of cancer and other proliferative disorders, we studied the signal transduction of DIFs in mammalian cells mainly using HeLa cells. Although the precise mechanisms underlying their antiproliferative effects are not yet known, we found that DIFs (DIF-1 and DIF-3) inhibited mammalian cell proliferation by suppressing the expression of cyclin D1 mRNA and protein through the activation of GSK-3$\beta$ (28 – 31).

DIFs dephosphorylated $Ser^9$ of GSK-3$\beta$ by an unknown mechanism and thus activated this kinase. Activated GSK-3$\beta$ by DIFs induced $\beta$-catenin degradation and suppressed $\beta$-catenin/TCF–dependent transcription activity, indicating that DIFs inhibit the Wnt/$\beta$-catenin signaling pathway. We also found that DIFs reduced the activity of a reporter gene driven by the human cyclin D1 promoter (+134/–961 bp) via a TCF binding site (–75/–81 bp) (29). This result suggests that DIFs inhibited cyclin D1 mRNA expression via the inhibition of $\beta$-catenin/TCF–dependent transcription

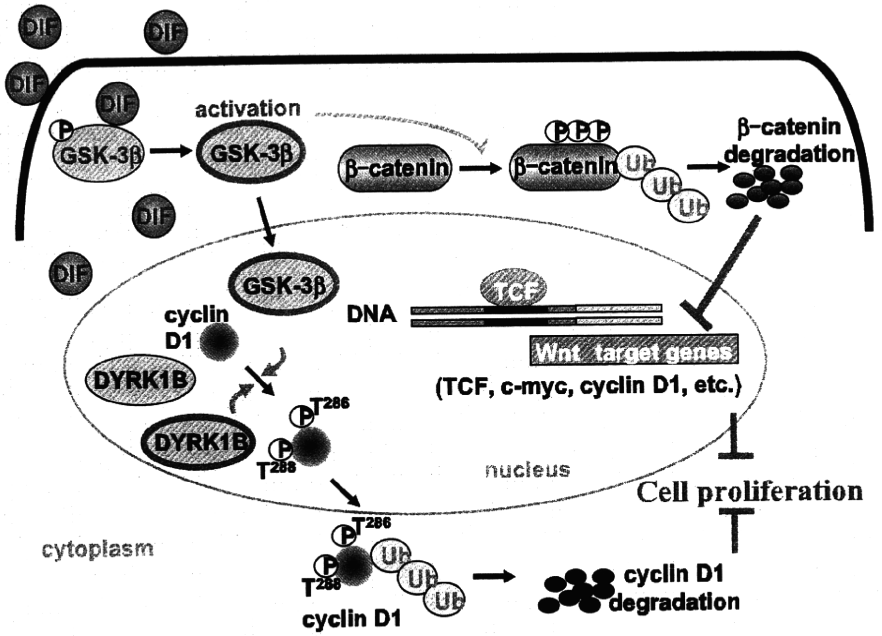


**Fig. 3.** DIFs action and the Wnt/$\beta$-catenin signaling pathway. DIFs enter into the cell and dephosphorylate GSK-3$\beta$ at $Ser^9$ by unknown mechanisms, resulting in the activation of this kinase. Activated-GSK-3$\beta$ translocates into nucleus and phosphorylates $Thr^{286}$ of cyclin D1. DIFs also activated DYRK1B, which is present in nucleus, by an unknown mechanism, and activated DYRK1B phosphorylates $Thr^{288}$ of cyclin D1. Phosphorylated cyclin D1 is exported from the nucleus, resulting in its degradation by the 26S proteasome system after ubiquitination. Activated-GSK-3$\beta$ also phosphorylates $\beta$-catenin in the cytoplasm. Phosphorylated $\beta$-catenin is degraded, resulting in the inhibition of transcription of the target genes, such as cyclin D1 and c-myc. GSK-3$\beta$, glycogen synthase kinase-3$\beta$; DYRK1B, dual-specificity tyrosine phosphorylation-regulated kinase 1B; Ub, ubiquitin.

activity. On the other hand, we also found that the activated GSK-3$\beta$ translocated to the nucleus and phosphorylated cyclin D1 on $Thr^{286}$ to trigger the degradation of cyclin D1 by an ubiquitin-dependent mechanism (28, 30, 31). Correlated with the above observations, DIFs induced G0/G1 cell cycle arrest, which was rescued by the overexpression of cyclin D1 (28), suggesting that DIFs were likely to induce cell cycle arrest by reducing the expression of cyclin D1.

Cyclin D1 degradation is facilitated by the phosphorylation of specific threonine residues, not only 286 but also 288, according to previous reports (20, 21, 32). Zou et al. (32) reported that dual-specificity tyrosine-phosphorylation–regulated kinase 1B (DYRK1B), a member of the DYRK family, phosphorylates cyclin D1 on $Thr^{288}$, also resulting in cyclin D1 degradation. Therefore, the effect of DIF-3 on DYRK1B was examined and it was found that not only GSK-3$\beta$ but also DYRK1B was involved in the phosphorylation of cyclin D1 to trigger its degradation (31). This may have an important implication in DIFs-induced cyclin D1 degradation because DIFs induce rapid and strong degradation of cyclin D1 (within 1 h). Clarified DIFs action is summarized in Fig. 3.

The antiproliferative effect of DIFs via strong reduction of the expression level of cyclin D1 is not limited to HeLa cells, but is also common to human squamous cell carcinoma cell lines (SAS and NA) (30), human colorectal carcinoma cell line (HCT-116), and human osteosarcoma cell line (SaOS-2) (author's unpublished observation). As described above, DIFs inhibit the Wnt/$\beta$-catenin signaling pathway via the activation of GSK-3$\beta$, whereas the target molecule is not clarified. Recently, Shimizu et al. reported that calmodulin-dependent cyclic nucleotide phosphodiesterase (PDE1) could be a pharmacological target molecule for DIF-1 (33). Although this protein might not be the molecule responsible for regulation of the antiproliferative effect of DIF-1 (4), some inhibitors for PDE1 are expected to be applicable to cancer (34, 35). Taken together, it seems likely that DIFs are potent antitumor agents, and identification of the target molecule(s) for DIFs may offer ideas for the design of new anticancer drugs.

## Conclusions

Cyclin D1 is a positive regulator of the cell cycle and promotes transition from the G1phase to the S phase in cooperation with CDK4 or 6. Amplification of the gene encoding cyclin D1 and overexpression of the cyclin D1 protein are frequently found in several types of human malignant neoplasms. GSK-3$\beta$ plays a critical role in the regulation of the amount of cyclin D1, as this kinase is involved in both cyclin D1 mRNA transcription and ubiquitin-dependent proteolysis. We found that DIFs act as an inhibitor of the Wnt/$\beta$-catenin signaling pathway via the activation of GSK-3$\beta$, whereas the target molecule is not clarified. Therefore, DIFs could be potent antitumor agents and identification of the target molecule(s) for DIFs may offer ideas for the design of new anticancer drugs.

## Acknowledgments

We would like to thank Prof. Yutaka Watanabe for providing DIFs. This work was supported by a Grant-in-Aid for Scientific Research from the Ministry of Education, Culture, Sports, Science, and Technology.

## References

1 Nelson WJ, Nusse R. Convergence of Wnt, β-catenin, and cadherin pathways. Science. 2004;303:1483–1487.
2 Moon RT, Bowerman B, Boutros M, Perrimon N. The promise and perils of Wnt signaling through β-catenin. Science. 2002; 296:1644–1646.
3 Akiyama T. Wnt/β-catenin signaling. Cytokine Growth Factor Rev. 2000;11:273–282.
4 Mlodzik M. Planar cell polarization: do the same mechanisms regulate Drosophila tissue polarity and vertebrate gastrulation? Trends Genet. 2002;18:564–571.
5 Kühl M, Sheldahl LC, Park M, Miller JR, Moon RT. The Wnt/$Ca^{2+}$ pathway: a new vertebrate Wnt signaling pathway takes shape. Trends Genet. 2000;16:279–283.
6 Chen AE, Ginty DD, Fan CM. Protein kinase A signalling via CREB controls myogenesis induced by Wnt proteins. Nature. 2005;433:317–322.
7 Cohen P, Frame S. The renaissance of GSK3. Nat Rev Mol Cell Biol. 2001;2:769–776.
8 Frame S, Cohen P. GSK3 takes centre stage more than 20 years after its discovery. Biochem J. 2001;359:1–16.
9 Cross D, Alessi DR, Cohen P, Andjelkovich M, Hemmings BA. Inhibition of glycogen synthase kinase-3 by insulin mediated by protein kinase B. Nature. 1995;378:785–789.
10 Kitagawa M, Hatakeyama S, Shirane M, Matsumoto M, Ishida N, Hattori K, et al. An F-box protein, FWD1, mediates ubiquitin-dependent proteolysis of β-catenin. EMBO J. 1999;18: 2401–2410.
11 Liu C, Li Y, Semenov M, Han C, Baeg GH, Tan Y, et al. Control of β-catenin phosphorylation/degradation by a dual-kinase mechanism. Cell. 2002;108:837–847.
12 Willert K, Jones KA. Wnt signaling: is the party in the nucleus? Genes Dev. 2006;20:1394–1404.
13 Sherr CJ. D-type cyclins. Trends Biochem Sci. 1995;20:187–190.
14 Sherr CJ. Cancer cell cycles. Science. 1996;274:1672–1677.
15 Barnes DM, Gillett CE. Cyclin D1 in breast cancer. Brest Cancer Res Treat. 1998;52:1–15.
16 Barbieri F, Lorenzi P, Ragni N, Schettini G, Bruzzo C, Pedullá F, et al. Overexpression of cyclin D1 is associated with poor survival in epithelial ovarian cancer. Oncology. 2004;66:310–315.
17 Utsunomiya T, Doki Y, Takemoto H, Shiozaki H, Yano M, Sekimoto M, et al. Correlation of β-catenin and cyclin D1 expression in colon cancers. Oncology. 2001;61:226–233.
18 Fu M, Wang C, Li Z, Sakamaki T, Pestell RG. Cyclin D1: normal and abnormal functions. Endocrinology. 2004;145:5439–5447.
19 Malumbres M, Barbacid M. To cycle or not to cycle: a critical decision in cancer. Nat Rev Cancer. 2001;1:222–231.
20 Diehl JA, Zindy F, Sherr CJ. Inhibition of cyclin D1 phosphorylation on threonine-286 prevents its rapid degradation via the ubiquitin-proteasome pathway. Genes Dev. 1997;11:957–972.
21 Diehl JA, Cheng M, Roussel MF, Sherr CJ. Glycogen synthase kinase-3β regulates cyclin D1 proteolysis and subcellular localization. Genes Dev. 1998;12:3499–3511.
22 Alt JR, Cleveland JL, Hannink M, Diehl JA. Phosphorylation-dependent regulation of cyclin D1 nuclear export and cyclin D1-dependent cellular transformation. Genes Dev. 2000;15:3102–3114.
23 Morris HR, Taylor GW, Masento MS, Jermyn KA, Kay RR. Chemical structure of the morphogen differentiation inducing factor from Dictyostelium discoideum. Nature. 1987;328:811–814.
24 Morris HR, Masento MS, Taylor GW, Jermyn KA, Kay RR. Structure elucidation of two differentiation inducing factors (DIF-2 and DIF-3) from the cellular slime mould Dictyostelium discoideum. Biochem J. 1988;249:903–906.
25 Asahi K, Sakurai A, Takahashi N, Kubohara Y, Okamoto K, Tanaka Y. DIF-1, morphogen of Dictyostelium discoideum, induces the erythroid differentiation in murine and human leukemia cells. Biochem Biophys Res Commun. 1995;208: 1036–1039.
26 Kubohara Y. DIF-1, putative morphogen of D. discoideum, suppresses cell growth and promotes retinoic acid-induced cell differentiation in HL-60. Biochem Biophys Res Commun. 1997;236:418–422.
27 Kubohara Y. Effects of differentiation-inducing factors of Dictyostelium discoideum on human leukemia K562 cells: DIF-3 is the most potent anti-leukemic agent. Eur J Pharmacol. 1999;381:57–62.
28 Takahashi-Yanaga F, Taba Y, Miwa Y, Kubohara Y, Watanabe Y, Hirata M, et al. Dictyostelium differentiation-inducing factor-3 activates glycogen synthase kinase-3β and degrades cyclin D1 in mammalian cells. J Biol Chem. 2003;278:9663–9670.
29 Yasmin T, Takahashi-Yanaga F, Mori J, Miwa Y, Hirata M, Watanabe Y, et al. Differentiation-inducing factor-1 suppresses gene expression of cyclin D1 in tumor cells. Biochem Biophys Res Commun. 2005;338:903–909.
30 Mori J, Takahashi-Yanaga F, Miwa Y, Watanabe Y, Hirata M, Morimoto S, et al. Differentiation-inducing factor-1 induces cyclin D1 degradation through the phosphorylation of $Thr^{286}$ in squamous cell carcinoma. Exp Cell Res. 2005;310:426–433.
31 Takahashi-Yanaga F, Mori J, Matsuzaki E, Watanabe Y, Hirata M, Miwa Y, et al. Involvement of GSK-3β and DYRK1B in differentiation-inducing factor-3-induced phosphorylation of cyclin D1 in HeLa cells. J Biol Chem. 2006;281:38489–38497.
32 Zou Y, Ewton DZ, Deng X, Mercer SE, Friedman E. Mirk/dyrk1B kinase destabilizes cyclin D1 by phosphorylation at threonine 288. J Biol Chem. 2004;279:27790–27798.
33 Shimizu K, Murata T, Tagawa T, Takahashi K, Ishikawa R, Abe Y, et al. Calmodulin-dependent cyclic nucleotide phosphodiesterase (PDE1) is a pharmacological target of differentiation-inducing factor-1, an antitumor agent isolated from Dictyostelium. Cancer Res. 2004;64:2568–2571.
34 Kakkar R, Raju RV, Sharma RK. Calmodulin-dependent cyclic nucleotide phosphodiesterase (PDE1). Cell Mol Life Sci. 1999; 55:1164–1186.
35 Lerner A, Kim DH, Lee R. The cAMP signaling pathway as a therapeutic target in lymphoid malignancies. Leuk Lymphoma. 2000;37:39–51.

Biochemical and Biophysical Research Communications 378 (2009) 851–856

Contents lists available at ScienceDirect

Biochemical and Biophysical Research Communications

journal homepage: www.elsevier.com/locate/ybbrc

# Knockout of the *l-pgds* gene aggravates obesity and atherosclerosis in mice

Reiko Tanaka [a,b], Yoshikazu Miwa [a,*], Kin Mou [a], Morimasa Tomikawa [c], Naomi Eguchi [d], Yoshihiro Urade [d], Fumi Takahashi-Yanaga [a], Sachio Morimoto [a], Norio Wake [b], Toshiyuki Sasaguri [a]

[a] *Department of Clinical Pharmacology, Faculty of Medical Sciences, Kyushu University, 3-1-1, Maidashi, Higashi-ku, Fukuoka 812-8582, Japan*
[b] *Department of Obstetrics and Gynecology, Faculty of Medical Sciences, Kyushu University, Fukuoka, Japan*
[c] *Department of Future Medicine and Innovative Medical Information, Faculty of Medical Sciences, Kyushu University, Fukuoka, Japan*
[d] *Department of Molecular Behavioral Biology, Osaka Bioscience Institute, Suita, Japan*

ARTICLE INFO

*Article history:*
Received 26 November 2008
Available online 12 December 2008

*Keywords:*
Lipocalin-type prostaglandin D synthase
Apolipoprotein E
Knockout mice
Atherosclerosis
Interleukin-1β
Monocyte chemoattractant protein type-1
Obesity

ABSTRACT

This study was designed to determine whether *lipocalin type-prostaglandin D synthase* (*l-pgds*) deficiency contributes to atherogenesis using gene knockout (KO) mice. A high-fat diet was given to 8-week-old C57BL/6 (wild type; WT), *l-pgds* KO (LKO), *apolipoprotein E* (*apo E*) KO (AKO) and *l-pgds*/*apo E* double KO (DKO) mice. The *l-pgds* deficient mice showed significantly increased body weight, which was accompanied by increased size of subcutaneous and visceral fat tissues. Fat deposition in the aortic wall induced by the high-fat diet was significantly increased in LKO mice compared with WT mice, although there was no significant difference between AKO and DKO mice. In LKO mice, atherosclerotic plaque in the aortic root was also increased and, furthermore, macrophage cellularity and the expression of pro-inflammatory cytokines such as interleukin-1β and monocyte chemoattractant protein-1 were significant increased. In conclusion, *l-pgds* deficiency induces obesity and facilitates atherosclerosis, probably through the regulation of inflammatory responses.



Lipocalin-type prostaglandin D synthase (L-PGDS) is the enzyme that converts $PGH_2$ into $PGD_2$ in the process of an arachidonic acid metabolism. The synthesized $PGD_2$ is further non-enzymatically metabolized to the $PGJ_2$ series including $PGJ_2$, $\Delta^{12}$-$PGJ_2$ and 15-deoxy-$\Delta^{12,14}$-$PGJ_2$ (15d-$PGJ_2$) [1]. Because L-PGDS is highly expressed in the central nervous system, its role in neurological disorders has been well studied [2–4]. In addition, recent studies have revealed that L-PGDS is constitutively expressed in the vascular endothelium [5] and that the downstream PGs, $PGD_2$ and the $PGJ_2$ series mainly act as protective factors for blood vessels [6]. The role of 15d-$PGJ_2$ has received particular attention because it was reported as a natural ligand of the nuclear receptor peroxisome proliferator-activated receptor-γ (PPARγ) that induces the differentiation of adipose cells and macrophages [7,8], which contribute to insulin resistance. 15d-$PGJ_2$ has been shown to be a unique material that is able to protect the vessel wall from injurious stimuli by controlling cell fate such as proliferation, differentiation and apoptosis, and by inhibiting inflammation in the vascular wall [6,9,10].

L-PGDS is secreted into the blood and urine, and several clinical studies have suggested a close association between L-PGDS levels and cardiovascular disease or its risk factors. The urinary L-PGDS level is significantly increased in patients with hypertension [11]. The L-PGDS concentration is increased in both serum and urine in diabetic patients and blood sugar control reversed the increase in urinary excretion of L-PGDS [12]. We previously reported that the serum L-PGDS level increases with aging and is associated with subclinical atherosclerosis as evaluated by the maximal intima–media complex thickness of the common carotid artery (C-IMT *max*) and by the pulse wave velocity [13]. In addition, we have identified single nucleotide polymorphisms (SNPs) in the *l-pgds* gene in Japanese people, and showed that a common SNP 4111A>C influences C-IMT *max* [14]. These observations strongly suggest the importance of L-PGDS in the pathogenesis of atherosclerosis; however, its role in vivo has not been well investigated.

Therefore, in the present study, to clarify the pathophysiologic role of L-PGDS in atherosclerosis, we investigated the effects of a high-fat diet on atherosclerosis and related parameters in *l-pgds* gene knockout (LKO) mice. We also crossed these mice with *apolipoprotein E (apo E)* knockout (AKO) mice, which are frequently used as a model of atherosclerosis, to generate a double knockout (DKO), and similarly investigated this phenotype.

## Methods

*Animals.* All animal experiments were approved by the Committee on the Ethics of Animal Experiments, Kyushu University Graduate School of Medical Sciences. LKO mice were generated as previously described [4]. AKO mice and C57BL/6 (wild type, WT)

* Corresponding author. Fax: +81 92 642 6084.
*E-mail address:* ymiwa@clipharm.med.kyushu-u.ac.jp (Y. Miwa).

0006-291X/$ - see front matter © 2008 Elsevier Inc. All rights reserved.
doi:10.1016/j.bbrc.2008.11.152

mice were obtained from Jackson Laboratory (Bar Harbor, ME). DKO mice were generated by mating LKO mice with AKO mice. After genotyping by polymerase chain reaction analysis, littermates from the F2 generation of this crossbreed were used to establish DKO mating, and the resulting progeny was used in our study. All animals were of pure (9-generation backcross) C57BL/6 genetic background. Male mice were fed a normal chow diet until 8 weeks of age, after which they received a high-fat diet containing 30% fat (Oriental Yeast Co., Tokyo, Japan) for 20 weeks. Mice were maintained in an air-conditioned room (25 °C; humidity 50%) with a 12 h light and dark cycle. Animals had free access to diet and drinking water but were not fed overnight prior to the experiments.

During the high-fat feeding, body weight and systolic blood pressure (BP) were measured every 4 weeks. Systolic BP was examined by tail-cuff plethysmography (BP98-A, Softron Co., Tokyo, Japan) on conscious restrained mice. Each measurement was performed five times, and values were averaged and recorded. Food intake was monitored daily for a period of 7 days in single-housed mice. After a week of acclimatization to the new environment, the amount of diet ingested was calculated as the difference between the weight of the food remaining in the food bin and the amount of pre-weighed food added the day before. Serum levels of cholesterols, triglyceride, creatinine and adiponectin were determined using blood samples collected from mice at 12 weeks after starting the high-fat diet.

Intraperitoneal glucose tolerance tests were performed in mice fasted for 16 h. Blood was collected before and after intraperitoneal injection of glucose (1 g/kg) at 15, 30, 60, 90 and 120 min. Intraperitoneal insulin tolerance test was performed after mice were fasted for 5 h. Blood glucose levels were measured prior to the injection of insulin (1.0 U/kg; Novolin®, Novo Nordisk Pharmaceuticals, Inc., Princeton, NJ) and at 15, 30, 60, 90 and 120 min after injection.

*Magnetic resonance imaging (MRI) studies.* In vivo MRI scanning was performed using a 0.3-T open MRI (AIRIS II, Hitachi Medico., Tokyo, Japan) to determine body fat distribution. Mice were anesthetized with pentobarbital (50 μg/g) and placed in a coil. T1-weighted SE sequence (TR/TE = 450/14 ms; FOV 85 mm; matrix 512 × 512; slice thickness 2 mm) was used to acquire 14 transverse slices. To evaluate the volumes of visceral and subcutaneous adipose tissue compartments, digital images were captured and hyper-intense fat was manually segmented and areas calculated as pixels using NIH Image J software (version 1.6.0, National Institute of Health, ML). The average values obtained from six consecutive slices between the middle of the right kidney to urinary bladder were defined as the fat tissue volume.

*Measurements of adipocyte sizes.* To determine adipocyte sizes of visceral and subcutaneous fat, the cross-sectional area of adipocytes was measured on paraffin-embedded hematoxylin–eosin-stained sections as previously described [15]. After converting the image of adipose tissue under the microscope to a binary image, each adipocyte from five randomly chosen fields (approximately 100 cells per mouse) was manually segmented and the areas calculated as pixels using NIH Image J software.

*En face evaluation of atherosclerotic lesions.* After the mice were fed with a high-fat diet for 20 weeks, they were anesthetized with pentobarbital and perfused with Krebs-Ringer solution, and the aorta was dissected from the aortic valve to the iliac bifurcation under a light microscope. The whole aorta was fixed in 10% formaldehyde for over 24 h, and opened longitudinally and pinned onto a black wax surface. To identify lipid-rich intraluminal lesions, the aorta was stained for 30 min in a saturated Oil-Red-O solution at room temperature. Digital images of the aortic lumen en face under the microscope were captured and saved on a computer and the index of atherosclerotic formation ([total lesion area/total surface area] × 100%) in the aortic arch was calculated for each aorta using NIH Image J software.

*Histological examination of the aortic root.* The aortic root was dissected and placed in 10% formaldehyde for 24 h and then transferred to 10–30% sucrose solution for 3 days. After embedding in OCT compound (Tissue-Tek), 10-μm-thick sections of the aortic roots were cut using a cryostat at −20 °C. Some of the sections were stained for 15 min in a saturated Oil-Red-O solution at room temperature and counterstained with hematoxylin. For quantitative estimation of the plaque contents, we analyzed the Oil-Red-O-stained areas as previously described [16] using NIH Image J software. The remaining sections were used for immunohistochemical analysis using the following antibodies: monoclonal anti-CD68 (AbD Serotec, Kidlington, UK), polyclonal anti-macrophage chemoattractant protein-1 (MCP-1) (sc-1785, Santa-Cruz, CA) and polyclonal anti-IL-1β (sc-7884; Santa-Cruz). After blocking endogenous peroxidase with 3% $H_2O_2$ in methanol for 30 min, serial 5-μm-thick cryosections of the aortic root were incubated with each antibody (1:100) overnight at 4 °C. The sections were treated with secondary biotinylated antibodies and incubated with streptavidin labeled with horseradish peroxidase using a Histofine SAB-PO Kit (Nichirei Co., Tokyo, Japan). The sections were then counterstained with hematoxylin. Under the microscope, percentages of stained cells from five randomly chosen fields were manually calculated.

*Statistical analysis.* Differences between groups were determined by two-tailed Student's *t*-test or one-way analysis of variance (ANOVA). When a significant difference was observed in ANOVA, the difference between two groups was analyzed by post hoc analysis. $P < 0.05$ was considered to be significant.

## Results

### *Effect of l-pgds deficiency on phenotype*

After the mice were fed a high-fat diet for 12 weeks from 8-weeks-old, the body weight of *l-pgds*-deficient (LKO and DKO) mice was significantly increased compared with the respective control (WT and AKO) mice (Table 1). When we compared diet consumption among the mice, food intake was significantly lower in *apo E*-deficient (AKO and DKO) mice compared with the WT and LKO mice, whereas *l-pgds* deficiency did not affect food intake. The body weight of *apo E*-deficient mice was also relatively lower but not statistically significant. Although the levels of systolic BP were not influenced by genotype, the serum levels of total cholesterol, LDL-cholesterol and triglyceride were significantly higher in *apo E*-deficient (AKO and DKO) mice. The *l-pgds* deficiency tended to increase total and LDL-cholesterol and triglyceride, although this was not statistically significant. HDL-cholesterol was relatively lower in DKO mice compared with AKO mice, but no difference was observed between WT and LKO mice. Because a recent report [17] showed that *l-pgds* KO mice become glucose intolerant and insulin resistant, we performed an intraperitoneal glucose tolerance test and insulin tolerance test. However, *l-pgds* deficiency did not significantly affect glucose or insulin tolerance (data not shown). Similarly, *l-pgds* deficiency did not affect the serum level of adiponectin, which is an insulin-sensitizing hormone that is exclusively expressed in adipose tissues (Table 1).

Next, to compare the fat tissue volume between *l-pgds*-deficient mice and control mice, we performed abdominal MRI using an open MRI scanner. As shown in Fig. 1A, we evaluated the volumes of visceral and subcutaneous adipose tissue compartments from six consecutive slices between the center of the right kidney (left) and the urinary bladder (right). Significant increases in volume of subcutaneous and visceral fat tissues were observed in MRI images in *l-pgds*-deficient (LKO and DKO) mice (Fig. 1B). These results

**Table 1**
Characteristics of mice (at 20-week-old).

| | WT | LKO | AKO | DKO |
|---|---|---|---|---|
| Number | 8 | 8 | 6 | 6 |
| Food intake (g/week) | 31 (1.0) | 30 (1.0) | 26 (1.5)* | 22 (0.7)* |
| Weight (g) | 37.1 (1.4) | 46.7 (1.9)* | 34.5 (1.2) | 40.7 (1.0)†* |
| Systolic blood pressure (mm Hg) | 104.6 (5.1) | 103.6 (7.3) | 101.6 (5.0) | 111.4 (7.0) |
| Total cholesterol (mg/dL) | 153.2 (17.2) | 189.2 (50.6) | 427.5 (77.7)* | 485.7(25.1)* |
| LDL-cholesterol (mg/dL) | 18.0 (3.0) | 24.5 (7.5) | 124.0 (23.1)* | 139.0 (3.6)* |
| HDL-cholesterol (mg/dL) | 61.6 (10.0) | 63.3 (8.1) | 45.5 (10.1) | 38.0 (3.8) |
| Triglyceride (mg/dL) | 12.3 (1.6) | 12.7 (2.2) | 48.3 (17.0)* | 68.0 (12.4)* |
| Adiponectin (mg/mL) | 9.6 (2.4) | 10.1 (2.6) | 17.3 (1.8)* | 18.4 (3.3) |

WT, wild type mice; LKO, *l-pgds* knockout mice; AKO, *apo E* knockout mice; DKO, *l-pgds/apo E* double knockout mice; LDL, low density lipoprotein; HDL, high density lipoprotein.
Data represent means (SE).
* $P < 0.05$ vs WT.
† $P < 0.05$ vs AKO.

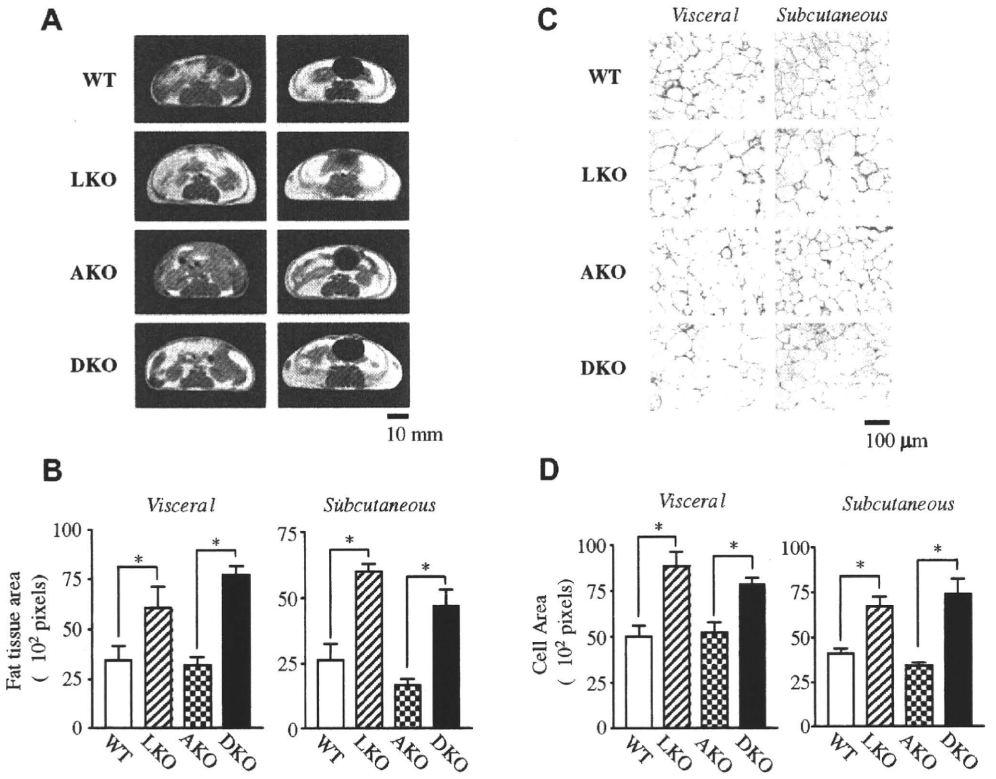


**Fig. 1.** (A) Abdominal open MRI transverse section of 20-week-old mice (maintained on a high-fat diet for 12 weeks). Left panel: center of the right kidney level; right panel: urinary bladder level. (B) Quantitative analyses of visceral and subcutaneous fat compartments. Areas of fat tissue were calculated as described in Methods. Data represent means ± SE ($n = 6$–8; *$P < 0.01$). (C) Representative hematoxylin–eosin-stained sections of visceral and subcutaneous fat in WT and LKO mice. Adipocyte sizes were calculated as described in Methods. Data represent means ± SE ($n = 6$; *$P < 0.01$).

were similar to the analysis of fat tissue weight obtained from sacrificed mice (data not shown).

We also compared the adipocyte sizes among mice. Adipocytes in visceral and subcutaneous fat isolated from *l-pgds*-deficient mice were significantly larger in size than those from WT and AKO mice (Fig. 1C and D).

*Effect of l-pgds deficiency on atherosclerosis*

Next, we evaluated the effect of *l-pgds* deficiency on atherosclerosis by investigating lipid depositions in the aortic wall and in cross-sections of the aortic root. As shown in Fig. 2A, Oil-Red-O staining in the longitudinally opened aortas showed a significant increase in atherosclerotic lesion area in LKO mice compared with WT mice after 20 weeks of high-fat diet feeding. Although greater increases in lipid deposition were observed in AKO and DKO mice, this was not statistically significant. Similarly, Oil-Red-O-stained atherosclerotic plaque area in the aortic root was increased in LKO mice compared with WT mice (Fig. 2B), but there was no difference between AKO and DKO mice (data not shown).

*Effects of l-pgds deficiency on inflammatory response*

The modulation of vascular remodeling mediated by inflammation is a key event in the progression of atherosclerosis. It has been reported that L-PGDS and its enzymatic products

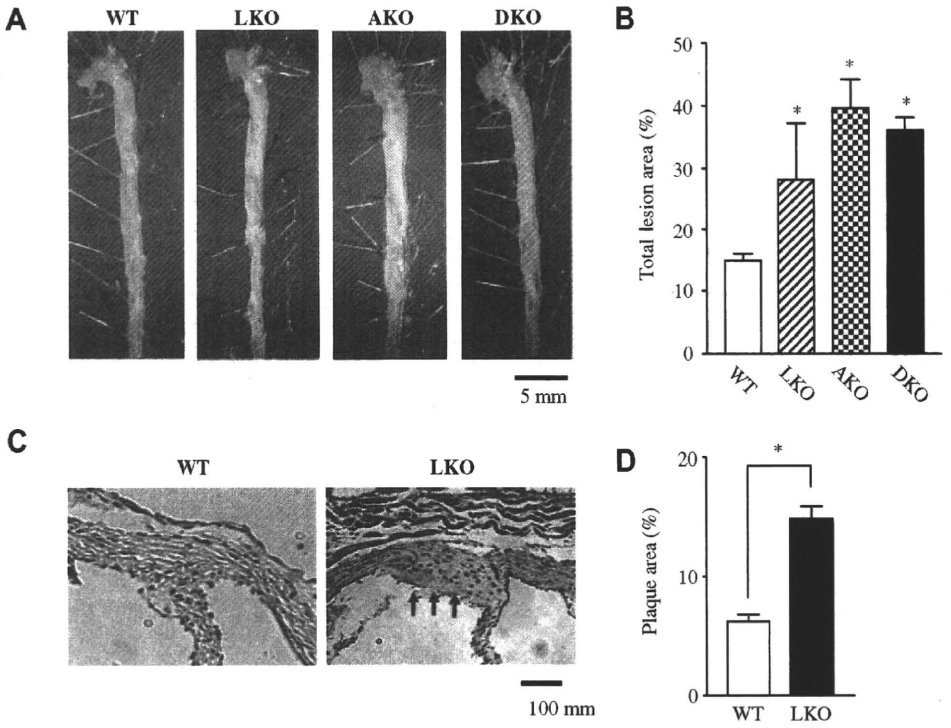


**Fig. 2.** Atherosclerotic lesions in 28-week-old mice (maintained on a high-fat diet for 20 weeks). (A) Lipid depositions in the aortic wall. Representative photomicrographs of longitudinally opened aortas between the subclavian and iliac branches stained with Oil-Red-O. (B) Quantitative analyses of lipid deposition in the aortic arch calculated as the percentage of the lesion area of the total vascular wall. Data represent means ± SE ($n = 6$; $^*P < 0.05$ vs WT). (C) Atherosclerotic lesions in the aortic root. Representative cross-sections of the aortic root stained with Oil-Red-O and hematoxylin in WT and LKO mice (arrows: lipid staining in red). (D) Quantitative analyses of atherosclerotic lesions calculated as the percentage of the Oil-Red-O stained area of the total aortic root. Data represent means ± SE for lesion area in five sections for each animal ($n = 6$; $^*P < 0.01$).

$PGD_2/PGJ_2$ have anti-inflammatory actions [7]. Therefore, to examine the effect of *l-pgds* deficiency on inflammation, we compared the infiltration of macrophages in the atherosclerotic lesions in aortic root sections between WT and LKO mice. The number of macrophages stained with anti-CD68 antibody was increased in LKO mice compared with WT mice (Fig. 3A). Furthermore, as shown in Fig. 3B, the expression of pro-inflammatory cytokines such as monocyte chemoattractant protein-1 (MCP-1) and interleukin-1β (IL-1β) in aortic root sections were also markedly enhanced in LKO mice.

## Discussion

Here, we showed that *l-pgds* deficiency increases body weight, which is accompanied with an increase in fat tissue volume in a high-fat environment. *l-pgds* deficiency also facilitates atherosclerosis, although this effect occurred to a lesser than in *apo E* deficiency.

The association between L-PGDS and obesity has not been well studied. However, several previous studies suggest that downstream PGs of L-PGDS, i.e., $PGD_2$ and $PGJ_2$ contribute to adipocyte differentiation or lipid metabolism, both of which are important in the pathogenesis of obesity through activation of PPARs. In particular, 15d-$PGJ_2$ stimulates the differentiation of adipose cells through PPARγ, which is abundantly expressed in adipocytes and functions as a key regulator of adipocyte differentiation. Considering these observations, the lack of *l-pgds* may inhibit downstream PG generation in adipose tissue, resulting in the enlargement of adipocytes and concomitant increase in fat tissue volume. Further studies are required to clarify the role of L-PGDS in the pathogenesis of obesity.

On the other hand, PPARγ plays a major role in insulin sensitivity. PPARγ increases small adipocytes by stimulating adipocyte differentiation and enhances expression of the insulin-sensitizing hormone adiponectin. A previous study [17] reported that LKO mice fed a diabetogenic diet were insulin resistant, glucose intolerant and had low serum adiponectin levels. In our study, the high-fat diet increased body weight and induced fat cell enlargement in LKO mice; however, it did not have a significant effect on insulin sensitivity or serum adiponectin levels. Although we are not able to fully explain this discrepancy, differences in diet compositions might be responsible for the inconsistent results. Very recently, the same group reported that L-PGDS stimulates glucose transport via enhanced translocation of the insulin-responsive glucose transporter GLUT4 [18]. However, since there are no other reports to have examined the effect of L-PGDS on glucose metabolisms, further studies are required to clarify this issue.

Because L-PGDS belongs to the lipocalin superfamily, a group of proteins that bind and transport small lipophilic molecules, L-PGDS may play a role in lipid transport. Indeed, we found an association between L-PGDS and serum lipid levels in the clinical studies. Serum L-PGDS levels were inversely associated with HDL-cholesterol [13] and a gene polymorphism of human *l-pgds* gene (4111 A>C) was associated with HDL-cholesterol levels [14]. In the present study, LKO mice showed relatively lower HDL-cholesterol and higher LDL-cholesterol levels, although these findings were not statistically significant. Based on these observations, even if L-PGDS contributes to lipid metabolism, its role does not seem to be important.

Our data also provide evidence for the atheroprotective functions of L-PGDS. Although the data were preliminary, Ragolia et al. [17] reported that LKO mice fed a diabetogenic diet showed

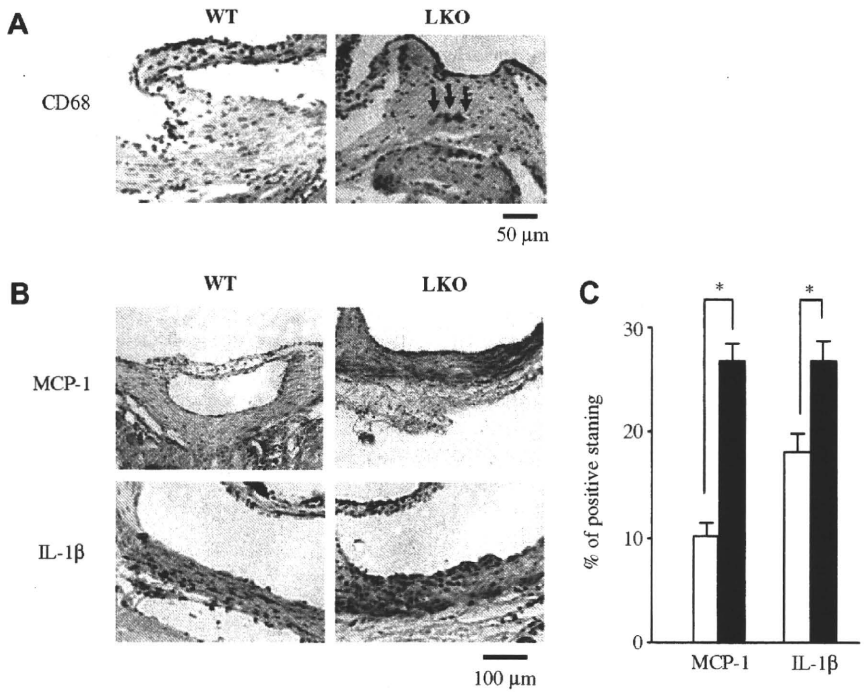


**Fig. 3.** (A) Immunohistochemical staining for CD68 in WT and LKO mice. Arrows indicate stained macrophages. (B) Immunohistochemical staining for MCP-1 and IL-1β in WT and LKO mice. (C) Quantitative analyses of the cell areas that stained positive for MCP-1 and IL-1β in WT mice (open bars) and LKO mice (closed bars). Data represent means ± SE for the percentage staining of the total plaque area in five sections for each animal ($n = 6$; $^{*}P < 0.01$).

progressed atherosclerosis. They attribute their results to differences in insulin resistance. Conversely, in our results, LKO mice fed a high-fat diet did not show differences in glucose homeostasis; however, they showed well-progressed atherosclerosis. Thus in our model, a mechanism other than insulin resistance seems to be associated with atherogenesis. One interesting possibility is the lack of a role of L-PGDS in inflammatory responses which play a central role in atherogenesis. The L-PGDS enzymatic product $PGD_2$ inhibits inducible nitric oxide synthase (NOS) [19] in vascular smooth muscle cells and suppresses the expression of pro-inflammatory mediators such as plasminogen activator inhibitor-1 [20] and vascular cell adhesion molecule-1 [21] in endothelial cells. 15d-$PGJ_2$ has also been shown to suppress inflammatory responses, which are dependent on or independent of PPARγ. 15d-$PGJ_2$ inhibits macrophage activation [22], production of monocyte inflammatory cytokines [23] and biologic functions of human natural killer cells [24]. 15d-$PGJ_2$ has also been shown to suppress inducible NOS expression [22]. In the present study, an increase in macrophage infiltration in the aortic root was observed in LKO mice. In support of this observation, the expression of MCP-1 which mediates monocyte recruitment to sites of inflammation and a pro-inflammatory cytokine, IL-1β, was enhanced in atherosclerotic lesions. These findings suggest that, in the vascular wall, *l-pgds* deficiency facilitates atherogenesis due to the lack of anti-inflammatory effects.

Taken together, we found that deletion of the *l-pgds* gene induces obesity in high cholesterol conditions in mice. *l-pgds* deficiency also resulted in highly progressed atherosclerosis by enhancing inflammatory responses. Our data suggest the potential anti-obese and atheroprotective effects of L-PGDS.

## Acknowledgments

We are grateful to Yuko Kubota for technical assistance. This study was supported by grants from the Ministry of Education, Culture, Sports, Science and Technology (Wakate B, No. 18790178) and Uehara Foundation.

## References

[1] Y. Kikawa, S. Narumiya, M. Fukushima, H. Wakatsuka, O. Hayaishi, 9-Deoxy-$\Delta^9,\Delta^{12\text{-}13,14}$-dihydroprostaglandin $D_2$, a metabolite of prostaglandin $D_2$ formed in human plasma, Proc. Natl. Acad. Sci. USA 81 (1984) 1317–1321.
[2] Y. Urade, O. Hayaishi, Prostaglandin $D_2$ and sleep regulation, Biochim. Biophys. Acta 1436 (1999) 606–615.
[3] O. Hayaishi, Y. Urade, Prostaglandin $D_2$ in sleep-wake regulation: recent progress and perspectives, Neuroscientist 8 (2002) 12–15.
[4] N. Eguchi, T. Minami, N. Shirafuji, Y. Kanaoka, T. Tanaka, A. Nagata, N. Yoshida, Y. Urade, S. Ito, O. Hayaishi, Lack of tactile pain (allodynia) in lipocalin-type prostaglandin D synthase-deficient mice, Proc. Natl. Acad. Sci. USA 96 (1999) 726–730.
[5] Y. Taba, T. Sasaguri, M. Miyagi, T. Abumiya, Y. Miwa, T. Ikeda, M. Mitsumata, Fluid shear stress induces lipocalin-type prostaglandin $D_2$ synthase expression in vascular endothelial cells, Circ. Res. 86 (2000) 967–973.
[6] T. Sasaguri, Y. Miwa, Prostaglandin $J_2$ family and the cardiovascular system, Curr. Vasc. Pharmacol. 2 (2004) 103–114 (Review).
[7] B.M. Forman, P. Tontonoz, J. Chen, R.P. Brun, B.M. Spiegelman, R.M. Evans, 15-Deoxy-$\Delta^{12,14}$-prostaglandin $J_2$ is a ligand for the adipocyte determination factor PPAR gamma, Cell 83 (1995) 803–812.
[8] S.A. Kliewer, J.M. Lenhard, T.M. Willson, I. Patel, D.C. Morris, J.M. Lehmann, A prostaglandin $J_2$ metabolite binds peroxisome proliferator-activated receptor gamma and promotes adipocyte differentiation, Cell 83 (1995) 813–819.
[9] Y. Miwa, T. Sasaguri, H. Inoue, Y. Taba, A. Ishida, T. Abumiya, 15-Deoxy-$\Delta^{12,14}$-prostaglandin $J_2$ induces $G_1$ arrest and differentiation marker expression in vascular smooth muscle cells, Mol. Pharmacol. 58 (2000) 837–844.
[10] Y. Miwa, F. Takahashi-Yanaga, S. Morimoto, T. Sasaguri, Involvement of clusterin in 15-deoxy-$\Delta^{12,14}$-prostaglandin $J_2$-induced vascular smooth muscle cell differentiation, Biochem. Biophys. Res. Commun. 319 (2004) 163–168.
[11] N. Hirawa, Y. Uehara, M. Yamakado, Y. Toya, T. Gomi, T. Ikeda, Y. Eguchi, M. Takagi, H. Oda, K. Seiki, Y. Urade, S. Umemura, Lipocalin-type prostaglandin d synthase in essential hypertension, Hypertension 39 (2002) 449–454.
[12] K. Hamano, Y. Totsuka, M. Ajima, T. Gomi, T. Ikeda, N. Hirawa, Y. Eguchi, M. Yamakado, M. Takagi, H. Nakajima, H. Oda, K. Seiki, N. Eguchi, Y. Urade, Y. Uehara, Blood sugar control reverses the increase in urinary excretion of prostaglandin D synthase in diabetic patients, Nephron 92 (2002) 77–85.
[13] Y. Miwa, H. Oda, Y. Shiina, K. Shikata, M. Tsushima, S. Nakano, T. Maruyama, S. Kyotani, N. Eguchi, Y. Urade, F. Takahashi-Yanaga, S. Morimoto, T. Sasaguri, Association of serum lipocalin-type prostaglandin D synthase levels with

subclinical atherosclerosis in untreated asymptomatic subjects, Hypertens. Res. 31 (2008) 1939–1947.
[14] Y. Miwa, S. Takiuchi, K. Kamide, M. Yoshii, T. Horio, C. Tanaka, M. Banno, T. Miyata, T. Sasaguri, Y. Kawano, Identification of gene polymorphism in lipocalin-type prostaglandin D synthase and its association with carotid atherosclerosis in Japanese hypertensive patients, Biochem. Biophys. Res. Commun. 322 (2004) 428–433.
[15] T. Björnheden, B. Jakubowicz, M. Levin, B. Odén, S. Edén, L. Sjöström, M. Lönn, Computerized determination of adipocyte size, Obes. Res. 12 (2004) 95–105.
[16] E.M. Rubin, R.M. Krauss, E.A. Spangler, J.G. Verstuyft, S.M. Clift, Inhibition of early atherogenesis in transgenic mice by human apolipoprotein AI, Nature 353 (1991) 265–267.
[17] L. Ragolia, T. Palaia, C.E. Hall, J.K. Maesaka, N. Eguchi, Y. Urade, Accelerated glucose intolerance, nephropathy, and atherosclerosis in prostaglandin $D_2$ synthase knock-out mice, J. Biol. Chem. 280 (2005) 29946–29955.
[18] L. Ragolia, C.E. Hall, T. Palaia, Lipocalin-type prostaglandin $D_2$ synthase stimulates glucose transport via enhanced GLUT4 translocation, Prostaglandins Other Lipid Mediat. 87 (2008) 34–41.
[19] H. Nagoshi, Y. Uehara, F. Kanai, S. Maeda, T. Ogura, A. Goto, T. Toyo-Oka, H. Esumi, T. Shimizu, M. Omata, Prostaglandin $D_2$ inhibits inducible nitric oxide synthase expression in rat vascular smooth muscle cells, Circ. Res. 82 (1998) 204–209.
[20] H. Negoro, W.S. Shin, R. Hakamada-Taguchi, N. Eguchi, Y. Urade, A. Goto, T. Toyo-Oka, T. Fujita, M. Omata, Y. Uehara, Endogenous prostaglandin $D_2$ synthesis reduces an increase in plasminogen activator inhibitor-1 following interleukin stimulation in bovine endothelial cells, J. Hypertens. 20 (2002) 1347–1354.
[21] H. Negoro, W.S. Shin, R. Hakamada-Taguchi, N. Eguchi, Y. Urade, A. Goto, T. Toyo-Oka, T. Fujita, M. Omata, Y. Uehara, Endogenous prostaglandin $D_2$ synthesis decreases vascular cell adhesion molecule-1 expression in human umbilical vein endothelial cells, Life Sci. 78 (2005) 22–29.
[22] M. Ricote, A.C. Li, T.M. Willson, C.J. Kelly, C.K. Glass, The peroxisome proliferator-activated receptor-gamma is a negative regulator of macrophage activation, Nature 391 (1998) 79–82.
[23] C. Jiang, A.T. Ting, B. Seed, PPAR-gamma agonists inhibit production of monocyte inflammatory cytokines, Nature 391 (1998) 82–86.
[24] X. Zhang, M.C. Rodriguez-Galan, J.J. Subleski, J.R. Ortaldo, D.L. Hodge, J.M. Wang, O. Shimozato, D.A. Reynolds, H.A. Young, Peroxisome proliferator-activated receptor-gamma and its ligands attenuate biologic functions of human natural killer cells, Blood 104 (2004) 3276–3284.

Biochemical and Biophysical Research Communications 377 (2008) 1185–1190

Contents lists available at ScienceDirect

Biochemical and Biophysical Research Communications

journal homepage: www.elsevier.com/locate/ybbrc

# Celecoxib-induced degradation of T-cell factors-1 and -4 in human colon cancer cells

Fumi Takahashi-Yanaga [a,*], Tatsuya Yoshihara [a], Kentaro Jingushi [a], Yoshikazu Miwa [a], Sachio Morimoto [a], Masato Hirata [b], Toshiyuki Sasaguri [a]

[a] Department of Clinical Pharmacology, Faculty of Medical Sciences, Kyushu University, Fukuoka, 812-8582, Japan
[b] Department of Molecular and Cellular Biochemistry, Faculty of Dental Sciences, Kyushu University, Fukuoka, 812-8582, Japan

ARTICLE INFO

*Article history:*
Received 9 October 2008
Available online 5 November 2008

*Keywords:*
Celecoxib
Wnt/β-catenin signaling pathway
T-cell factor (TCF)
Colon cancer cell

ABSTRACT

We examined the effect of celecoxib on the expression of T-cell factors (TCFs) to clarify the mechanism by which celecoxib suppress β-catenin/TCF-dependent transcriptional activity without reducing the level of β-catenin protein, using HCT-116 cells. Celecoxib suppressed the expression of TCF-1 and TCF-4 in a time-dependent manner. Pretreatment of cells with the proteasome inhibitor MG132 inhibited the loss of TCF-1 and TCF-4 induced by celecoxib, suggesting that celecoxib induced the proteasome-dependent degradation of TCF-1 and TCF-4. β-Catenin/TCF-dependent transcriptional activity was significantly decreased after the treatment with celecoxib for 6 h and the pretreatment of the cells with MG132 attenuated the effect of celecoxib. Further, celecoxib also suppressed the expression of TCF-1 and TCF-4 in another colon cancer cell line, DLD-1. Our results suggest that TCF-1 and TCF-4 degradation may involve the inhibition of the Wnt/β-catenin signaling pathway induced by celecoxib.



Most colorectal cancers have somatic mutations in adenomatous polyposis coli (APC) or β-catenin, which are members of the Wnt/β-catenin signaling pathway [1–4]. Although this pathway is essential to regulate gene transcription during embryo development, it is probably present in intestinal crypts throughout adult life, maintaining the balance between cell proliferation and differentiation [5,6]. The activity of this signaling pathway is determined by the amount of β-catenin in the cytoplasm. Normally, the cytoplasmic β-catenin level is kept low through continuous ubiquitin-proteasome-mediated degradation of β-catenin, which is regulated by a multiprotein complex (β-catenin destruction complex) containing axin, APC, glycogen synthase kinase-3β, and casein kinase 1α [7,8]. Mutations in APC and β-catenin retard β-catenin degradation by this system leading to accumulation of β-catenin in the cytoplasm and its translocation into the nucleus, resulting in the up-regulation of Wnt/β-catenin signaling pathway target genes together with T-cell factor (TCF). It has been reported that constant activation of this signaling pathway can lead to cancer.

Numerous experimental and epidemiological studies in humans suggest that aspirin and other nonsteroidal anti-inflammatory drugs (NSAIDs) have chemopreventive activity against colon cancer [9–11]. Several randomized trials have shown the growth inhibition of polyps and a decrease in the number of existing polyps in patients with familial adenomatous polyposis (FAP) who received sulindac or celecoxib [12,13]. Two randomized placebo-controlled studies have shown that aspirin reduced the risk of colorectal adenomas among individuals with previous colorectal cancer and adenoma, excluding FAP patients [14,15]. The possible cellular mechanisms underlying these chemopreventive effects of NSAIDs have been thought to be the induction of apoptosis, cell-cycle arrest and the inhibition of angiogenesis [10,11]. Moreover, NSAIDs have been reported to inhibit the Akt [16,17] and the Wnt/β-catenin signaling pathways [18–21].

Celecoxib is the only NSAID approved by the Food and Drug Administration for the treatment of FAP patients. However, the molecular mechanism responsible for the chemopreventive effect of celecoxib is not entirely understood. Although this compound was developed as a selective cyclooxygenase-2 (COX-2) inhibitor, additional pharmacological activities have emerged outside of its cox-2 inhibition. Celecoxib has potency to inhibit COX-2 activity at nanomolar range, however, it requires micromolar range to inhibit cellular proliferation and survival [22,23]. We previously reported that celecoxib inhibited β-catenin/TCF-dependent transcriptional activity without affecting the amount of β-catenin protein using HCT-116 cells which lack COX-2 expression, suggesting that this effect was COX-2-independent [24]. Recently, it has been reported that the TCF transcription factors TCF-4 and LEF-1 are ubiquitylated and degraded via the proteasome system [25]. Therefore, we examined the effect of celecoxib on TCF-1 and TCF-4 expression levels to identify the mechanism by which celecoxib reduces β-catenin/TCF-dependent transcriptional activity.

* Corresponding author. Fax: +81 92 642 6084.
*E-mail address:* yanaga@clipharm.med.kyushu-u.ac.jp (F. Takahashi-Yanaga).

0006-291X/$ - see front matter © 2008 Elsevier Inc. All rights reserved.
doi:10.1016/j.bbrc.2008.10.115

Our results suggested that celecoxib induces TCF-1 and TCF-4 degradation via the proteasome system without affecting β-catenin protein amount in the colon cancer cell lines HCT-116 and DLD-1. To our knowledge, this is the first report to show celecoxib induce the degradation of TCF family members.

## Materials and methods

*Chemicals and antibodies.* TOPflash (a TCF reporter plasmid) and FOPflash (a negative control for TOPflash) were purchased from Upstate Biotechnology. The monoclonal anti-GAPDH antibody was from Abcam. The monoclonal anti-TCF-4 antibody (6H5-3) was from Cell Signaling Technology (Danvers, MA). The polyclonal anti-TCF-1 (H-18) antibody was from Santa Cruz Biotechnology. The monoclonal anti-β-catenin antibody was from BD Biosciences. MG132 was from Peptide Institute (Osaka, Japan). Celecoxib was kindly provided by Pfizer.

*Cell culture.* HCT-116 cells, a human colon cancer cell line expressing wild-type APC and mutated β-catenin but lacking COX-2 [1,26–28], and DLD-1 cells, a human colon cancer cell line expressing mutated APC and wild-type β-catenin but lacking COX-2 [2,28,29], were grown in Dulbecco's modified Eagle's medium (Sigma) supplemented with 10% fetal bovine serum (FBS), 100 U/ml of penicillin G, and 0.1 μg/ml of streptomycin.

*Immunoblotting.* Immunoblotting analysis was performed as described previously [30]. Briefly, samples (10 μg/lane) were separated by 12% SDS–polyacrylamide gel electrophoresis (SDS–PAGE) and transferred to a polyvinylidene difluoride membrane using a semi-dry transfer system (1 h, 12 V). After blocking with 5% skim milk for 1 h, the membrane was probed with a first antibody. The membrane was washed three times and incubated with horseradish peroxidase-conjugated anti-rabbit or anti-mouse IgG (Cell Signaling Technology) for 1 h. Immunoreactive proteins on the membrane were visualized by treatment with a detection reagent (LumiGLO, Cell Signaling Technology). An optical densitometric scan was performed using Science Lab 99 Image Gauge Software (Fuji Photo Film).

*Luciferase reporter assay.* Cells were transfected with luciferase reporter plasmid (TOPflash or FOPflash) and pRL-SV40, a *Renilla* luciferase expression plasmid for the control of transfection efficiency, using Lipofectamine Plus reagent (Invitrogen). Cells were cultured for 24 h after transfection and stimulated with celecoxib (100 μM) for the period indicated. To evaluate the effect of MG132 on celecoxib action, transfected cells were treated with 10 μM of MG132 for 1 h and then stimulated with celecoxib for 6 h. Luciferase activity was determined with a luminometer (Lumat LB 9507, Berthold Technologies) and normalized with respect to *Renilla* luciferase activity.

*Statistical analysis.* The results are expressed as means ± SE. Statistical analysis of differences between two means was performed using the Student's *t*-test.

## Results

### *Celecoxib induces TCF-1 and TCF-4 protein degradation in HCT-116 cells*

We first examined whether celecoxib affects TCF-1 and TCF-4 expression in the human colon cancer cell line HCT-116. Cells were incubated with or without celecoxib for the indicated period, and the expression levels of TCF-1 and TCF-4 were examined by immunoblotting. Two bands were detected by antibody against TCF-1 and upper band was interpreted as non-specific bands from their molecular weight. The protein amounts of both TCF-1 and TCF-4 gradually increased with incubation period in control cells. On the other hand, the both protein amounts in 100 μM celecoxib-treated cells were significantly reduced after a 3-h treatment (Fig. 1A). Although we previously reported that celecoxib induced apoptosis in human colon cancer cell lines, degradation of TCF transcription factors induced by celecoxib was unlikely to be caused by cytotoxicity, because caspase-3 activity was not increased after 6-h treatment [24]. As shown in Fig. 1B, celecoxib decreased in the levels of TCF-1 and TCF-4 at 100 μM whereas it did not have significant effect until 50 μM. Thus, celecoxib reduced the protein levels of both TCF-1 and TCF-4 in a time-dependent manner at a concentration of 100 μM. We next examined the effect of the proteasome inhibitor MG132 on celecoxib-induced reduction of TCF-1 and TCF-4. Cells were treated with or without 10 μM MG132 for 1 h and stimulated with or without 100 μM celecoxib for 6 h. As shown in Fig. 2, pretreatment with MG132 significantly attenuated the effect of celecoxib, indicating that celecoxib accelerated the proteasome-dependent degradation of TCF-1 and TCF-4 in HCT-116 cells.

### *Celecoxib reduces β-catenin/TCF-dependent transcriptional activity*

Subsequently, the effect of celecoxib on the expression level of β-catenin was examined using HCT-116 cells, which has been reported to express stable β-catenin due to the mutation [1,26–28]. As shown in Fig. 3A, celecoxib did not affect the amount of β-catenin protein in the first 24 h of incubation and this result is well correlated with our previous report [24]. The effect of celecoxib on β-catenin/TCF-dependent transcriptional activity was examined using TCF reporter plasmid TOPflash and its negative control FOPflash. Celecoxib reduced TOPflash activity in a time-dependent manner without affecting FOPflash activity (Fig. 3B). Although we found that celecoxib significantly reduced the protein levels of TCF-1 and TCF-4 after a 3-h incubation, TOPFlash activity was not significantly affected after a 3-h incubation. Celecoxib gradually reduced the TOPFlash activity after a 6-h treatment. These results suggested that celecoxib might reduce β-catenin/TCF-dependent transcriptional activity due to the degradation of TCF transcription factors, and that this effect was independent of the β-catenin protein level. To clarify this point, we next examined the effect of celecoxib on β-catenin/TCF-dependent transcriptional activity using proteasome inhibitor MG132. For this purpose, transfected HCT-116 cells were pretreated with 10 μM of MG132 for 1 h and stimulated with celecoxib for 12 h. However, all most all cells treated with MG132 were died at the end of incubation period due to the cytotoxic effect of proteasome inhibitor (data not shown). Therefore, incubation period was shortened and the effect of celecoxib was evaluated after a 6-h treatment. As shown in Fig. 3C, although celecoxib significantly inhibited TOPFlash activity after a 6-h treatment, pretreatment with MG132 attenuated the effect of celecoxib. These results clearly indicated that the reduction of the β-catenin/TCF-dependent transcriptional activity was due to the degradation of TCF transcription factors.

### *Effect of celecoxib on TCF-1 and TCF-4 protein amounts in another colon cancer cell line, DLD-1*

The effect of celecoxib was also examined using the human colon cancer cell line DLD-1, which has mutation in APC and β-catenin degradation system is retarded [2,28]. As we previously reported that the same concentrations of celecoxib used in HCT-116 cells did not have significant effects on this cell line, we used a higher concentration of celecoxib (200 μM) for this experiment. As shown in Fig. 4A, 200 μM celecoxib greatly reduced the amounts of TCF-1 and TCF-4 proteins in a time-dependent manner, but had no significant effect on the expression of β-catenin in DLD-1 cells. Moreover, pretreatment with proteasome inhibitor MG132,

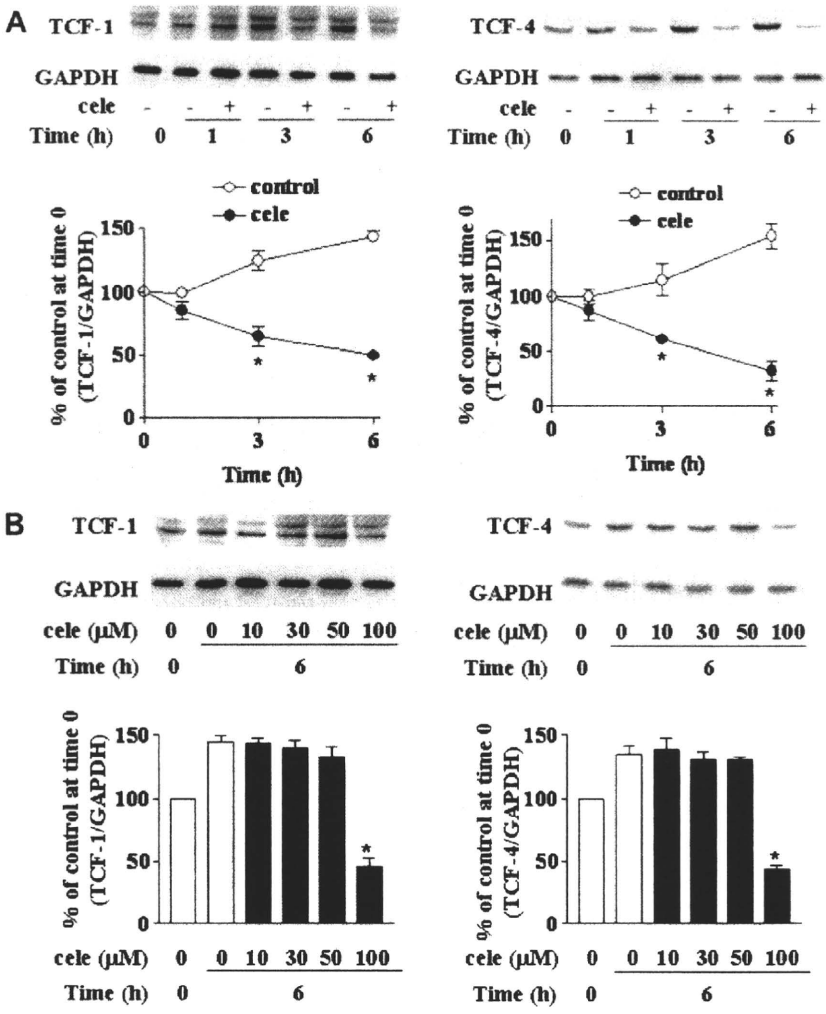


**Fig. 1.** The effect of celecoxib on the expression of TCF-1 and TCF-4. (A) Time course. HCT-116 cells were incubated with or without celecoxib (100 μM) for the period indicated. Protein samples were collected and separated by 12% SDS–PAGE and immunoblotted with the anti-TCF-1 antibody (left) or anti-TCF-4 antibody (right). (B) Dose dependency. HCT-116 cells were incubated with or without various amounts of celecoxib for 6 h. Protein samples were collected and separated by 12% SDS–PAGE and immunoblotted with the anti-TCF-1 antibody (left) or anti-TCF-4 antibody (right). The membrane was reprobed with anti-GAPDH antibody. The levels of protein bands were quantified and normalized to those of GAPDH. The results are shown as a percentage of the control level at time 0. Values are the means ± SE of three independent experiments. $^{*}p < 0.01$ vs. control (Student's *t*-test), cele: celecoxib.

inhibited the effect of celecoxib, indicating that celecoxib accelerated the proteasome-dependent degradation of TCF-1 and TCF-4 in DLD-1 cells (Fig. 4B). Taken together, these results indicated that celecoxib induced proteasome-dependent degradation of TCF-1 and TCF-4 in colon cancer cell lines, while the sensitivity to celecoxib is different among cell lines.

## Discussion

In this study, we showed that celecoxib induced the degradation of TCF-1 and TCF-4 in human colon cancer cell lines. Constitutive activation of the Wnt/β-catenin signaling pathway could trigger the formation of colon cancers. Activation of this pathway is due to genetic mutations that stabilize the β-catenin protein, allowing it to accumulate in the nucleus and form complexes with TCF transcription factors to activate the transcription of target genes. It has been proposed that abnormal expression levels or patterns of the target genes such as MYC, CCND1 and MMP7 have a role in tumor progression [1–4]. Therefore, anticancer drugs that suppress the transcriptional activity of the Wnt/β-catenin signaling pathway could be of important therapeutic value against colon cancers. Although one well known mechanism for suppressing the transcriptional activity of Wnt/β-catenin signaling pathway is β-catenin degradation, it is quite difficult to induce the degradation of β-catenin in most colon cancer cells due to mutations in β-catenin or components of the β-catenin destruction complex (including axin and APC), as described above. However, as shown in this study, celecoxib induced degradation of TCF transcription factors and inhibited the transcriptional activity of the Wnt/β-catenin signaling pathway. This might represent a new mechanism for inhibiting the transcriptional activity of the Wnt/β-catenin signaling pathway.

COX-2 is the key enzyme in the conversion of arachidonic acid to prostaglandins which promote cell proliferation, angiogenesis and inhibit the induction of apoptosis; therefore, the chemopreventive effect of NSAIDs is thought to be attributed to their COX-2 inhibitory activity. However, some studies have suggested that celecoxib has anticarcinogenic effects in cells which do not express COX-2 and COX-2-deficient tumors in a nude mice model [26,27]. In fact, the HCT-116 cells and DLD-1 cells used in this experiment

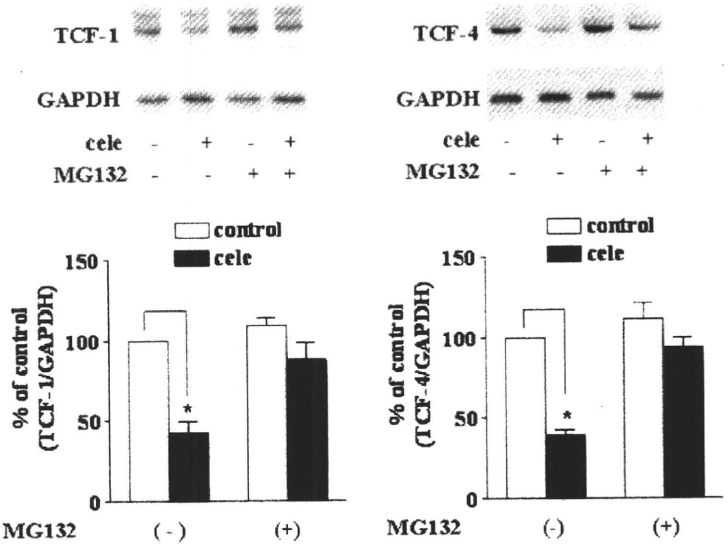


**Fig. 2.** Effect of the proteasome inhibitor MG132. HCT-116 cells were incubated with or without 10 μM MG132 for 1 h and stimulated with or without celecoxib (100 μM) for 6 h. Protein samples were collected and separated by 12% SDS–PAGE and immunoblotted with the anti-TCF-1 antibody (left) or anti-TCF-4 antibody (right). The membrane was reprobed with the anti-GAPDH antibody. The levels of protein bands were quantified and normalized to those of GAPDH. The results are shown as a percentage of the control level. Values are the means ± SE of three independent experiments performed in duplicate. $^{*}p < 0.01$ vs. control (Student's *t*-test), cele: celecoxib.

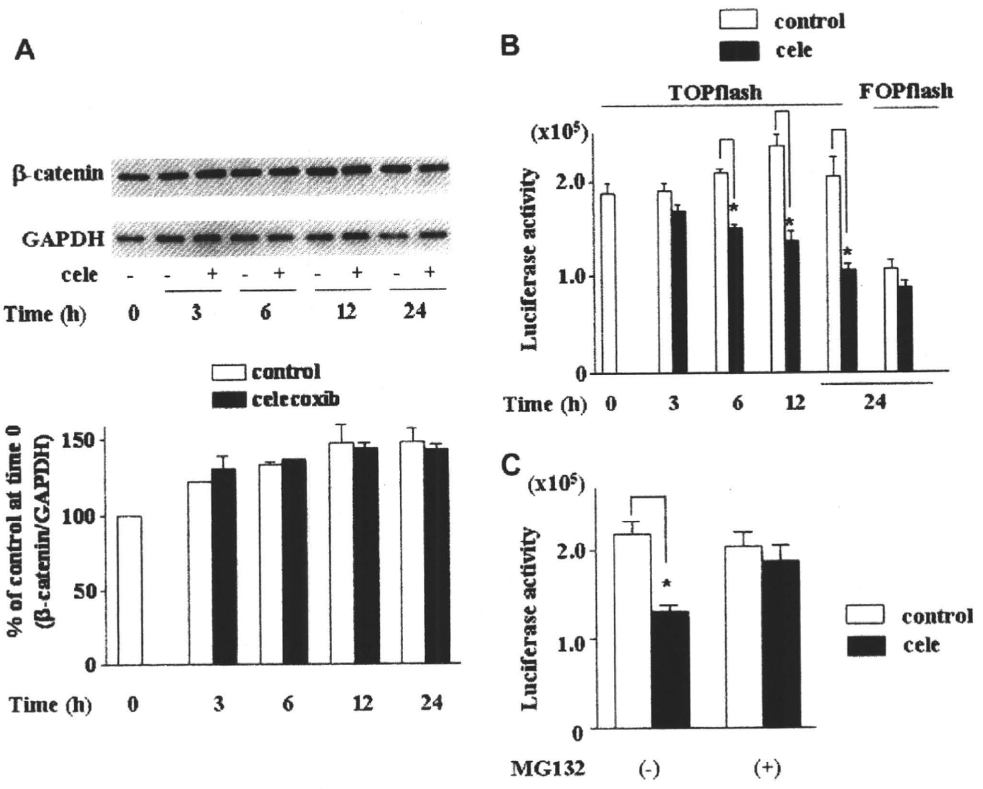


**Fig. 3.** The effect of celecoxib on β-catenin/TCF-dependent transcriptional activity. (A) Western blot analysis for β-catenin. HCT-116 cells were incubated with or without celecoxib (100 μM) for the period indicated. Protein samples were collected and separated by 12% SDS–PAGE and immunoblotted with the anti-β-catenin antibody. The membrane was reprobed with the anti-GAPDH antibody. The levels of protein bands were quantified and normalized to those of GAPDH. The results are shown as a percentage of the control level at time 0. Values are the means ± SE of three independent experiments. (B) Reporter gene assay with TOPFlash and FOPFlash. TOPflash or FOPflash was co-transfected with pRL-SV40 into HCT-116 cells. After 24-h incubation, cells were stimulated with or without celecoxib (100 μM) for the period indicated. Values are the means ± SE of three independent experiments performed in duplicate. $^{*}p < 0.01$ vs. control (Student's *t*-test). (C) MG132 inhibited the effect of celecoxib. TOPflash was co-transfected with pRL-SV40 into HCT-116 cells. After a 24-h incubation, cells were pretreated with or without 10 μM of MG132 for 1 h and then stimulated with or without 100 μM of celecoxib for 6 h. Values are the means ± SE of three independent experiments performed in duplicate. $^{*}p < 0.01$ vs. control (Student's *t*-test), cele: celecoxib.

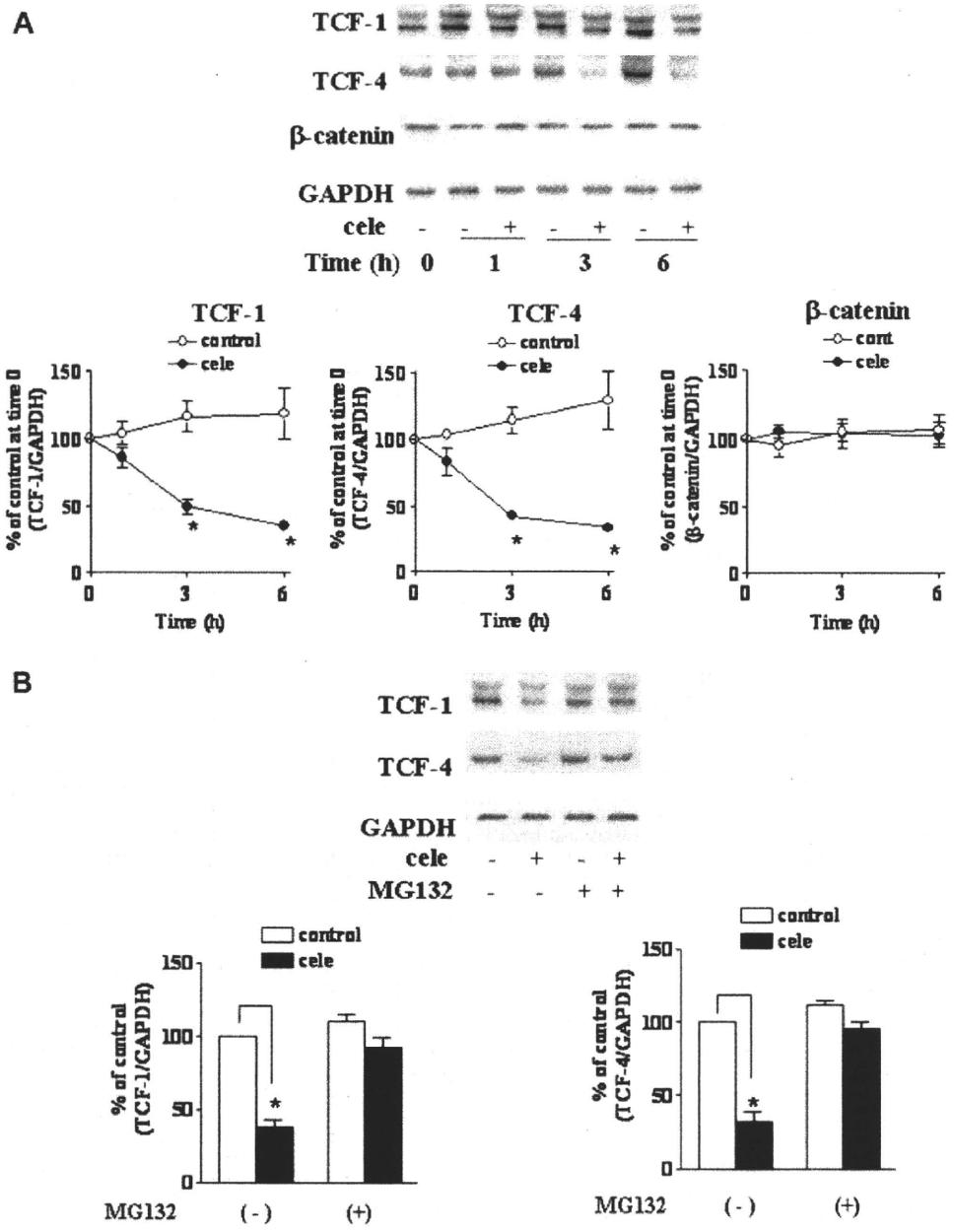


**Fig. 4.** The effect of celecoxib on the expression of TCF-1 and TCF-4 in DLD-1 cells. (A) Effect of celecoxib on TCFs expression in DLD-1 cells. DLD-1 cells were incubated with or without celecoxib (200 μM) for the indicated period. Protein samples were collected and separated by 12% SDS–PAGE and immunoblotted with anti-TCF-1, anti-TCF-4, anti-β-catenin and anti-GAPDH antibodies. The levels of protein bands were quantified and normalized to those of GAPDH. (B) MG132 inhibits TCFs degradation induced by celecoxib. HCT-116 cells were incubated with or without 10 μM MG132 for 1 h and stimulated with or without celecoxib (200 μM) for 6 h. Protein samples were collected and separated by 12% SDS–PAGE and immunoblotted with anti-TCF-1, anti-TCF-4, anti-β-catenin and anti-GAPDH antibodies. The levels of protein bands were quantified and normalized to those of GAPDH. The results are shown as a percentage of the control level. Values are the means ± SE of three independent experiments. $^{*}p < 0.01$ vs. control (Student's *t*-test), cele: celecoxib.

are known as COX-2-deficient cell lines [26,27], and not only COX-2 inhibitor but also COX-1 inhibitor (SC-560) induced degradation of TCF-1 and TCF-4. Thus celecoxib could induce degradation of TCF family members via COX-2-independent mechanisms.

There are at least 16 different variants of TCF-1, the molecular weights of which from 28 to 54 kDa, due to alternative splicing and promoter usage [31,32]. Half of them have a β-catenin binding domain (1–50 bp) (L-type, 1L–8L variants) which work as β-catenin/TCF-dependent transcriptional activators and the other half fail to bind β-catenin, because they lack the N-terminal region (1–114 bp) (S-type, 1S–8S variants), and act as a dominant-negative form of TCF-1 to inhibit β-catenin/TCF-dependent transcriptional activity [33,34]. Therefore, it might be important to clarify if celecoxib induces both L-type and S-type degradation. Although we could not clearly address which variant of the TCF-1 we detected at present, we might only be able to detect L-type variants of TCF-1 because of the anti-TCF-1 antibody we used is raised against the N-terminal region. In the case of TCF-4, there are 10 variants, molecular weights of which from 50 to 68 kDa, and all of which can bind to β-catenin to act as β-catenin/TCF-dependent transcriptional activators [35]. As 5 of 10 variants have almost same molecular weight (approx. 67 kDa) and the antibody we used could

recognize all variants, we are uncertain which TCF-4 variant we detected in HCT-116 and DLD-1 cells.

In summary, our results indicated that celecoxib induces degradation of TCF-1 and TCF-4 transcription factors and suppresses the transcriptional activity of the Wnt/β-catenin signaling pathway without affecting the level of β-catenin protein in colon cancer cells.

## References


[1] P.J. Morin, A.B. Sparks, V. Korinek, N. Barker, H. Clevers, B. Vogelstein, K.W. Kinzler, Activation of β-catenin-Tcf signaling in colon cancer by mutations in β-catenin or APC, Science 275 (1997) 1787–1790.

[2] A.B. Sparks, P.J. Morin, B. Vogelstein, K.W. Kinzler, Mutational analysis of the APC/β-catenin/Tcf pathway in colorectal cancer, Cancer Res. 58 (1998) 1130–1134.

[3] M. Bienz, H. Clevers, Linking colorectal cancer to Wnt signaling, Cell 103 (2000) 311–320.

[4] S. Segditsas, I. Tomlinson, Colorectal cancer and genetic alterations in Wnt pathway, Oncogene 25 (2006) 7531–7537.

[5] T. Reya, H. Clevers, Wnt signalling in stem cells and cancer, Nature 434 (2005) 843–850.

[6] J. Taipale, P.A. Beachy, The hedgehog and Wnt signalling pathways in cancer, Nature 411 (2001) 349–354.

[7] M. Kitagawa, S. Hatakeyama, M. Shirane, M. Matsumoto, N. Ishida, K. Hattori, I. Nakamichi, A. Kikuchi, K. Nakayama, K. Nakayama, An F-box protein, FWD1, mediates ubiquitin-dependent proteolysis of β-catenin, EMBO J. 18 (1999) 2401–2410.

[8] C. Liu, Y. Li, M. Semenov, C. Han, G.H. Baeg, Y. Tan, Z. Zhang, X. Lin, X. He, Contorl of β-catenin phosphorylation/degradation by a dual-kinase mechanism, Cell 108 (2002) 837–847.

[9] M.J. Thun, M.M. Namboodiri, C.W. Jr. Heath, Aspirin use and reduced risk of fatal colon cancer, N. Engl. J. Med. 325 (1991) 1593–1596.

[10] T.A. Chan, Nonsteroidal anti-inflammatory drugs, apoptosis, and colon-cancer chemoprevention, Lancet Oncol. 3 (2002) 166–174.

[11] M.J. Thun, S.J. Henley, C. Patrono, Nonsteroidal anti-inflammatory drugs as anticancer agents: mechanistic, pharmacologic, and clinical issues, J. Natl. Cancer Inst. 94 (2002) 252–266.

[12] F.M. Giardiello, S.R. Hamilton, A.J. Krush, S. Piantadosi, L.M. Hylind, P. Celano, S.V. Booker, C.R. Robinson, G.J. Offerhaus, Treatment of colonic and rectal adenomas with sulindac in familial adenomatous polyposis, N. Engl. J. Med. 328 (1993) 1313–1316.

[13] G. Steinbach, P.M. Lynch, R.K. Phillips, M.H. Wallace, E. Hawk, G.B. Gordon, N. Wakabayashi, B. Saunders, Y. Shen, T. Fujimura, L.K. Su, B. Levin, The effect of celecoxib, a cyclooxygenase-2 inhibitor, in familial adenomatous polyposis, N. Engl. J. Med. 342 (2000) 1946–1952.

[14] R.S. Sandler, S. Halabi, J.A. Baron, S. Budinger, E. Paskett, R. Keresztes, N. Petrelli, J.M. Pipas, D.D. Karp, C.L. Loprinzi, G. Steinbach, R. Schilsky, A randomized trial of aspirin to prevent colorectal adenomas in patients with previous colorectal cancer, N. Engl. J. Med. 348 (2003) 883–890.

[15] J.A. Baron, B.F. Cole, R.S. Sandler, R.W. Haile, D. Ahnen, R. Bresalier, G. McKeown-Eyssen, R.W. Summers, R. Rothstein, C.A. Burke, D.C. Snover, T.R. Church, J.I. Allen, M. Beach, G.J. Beck, J.H. Bond, T. Byers, E.R. Greenberg, J.S. Mandel, N. Marcon, L.A. Mott, L. Pearson, F. Saibil, R.U. van Stolk, A randomized trial of aspirin to prevent colorectal adenomas, N. Engl. J. Med. 348 (2003) 891–899.

[16] S. Arico, S. Pattingre, C. Bauvy, P. Gane, A. Barbat, P. Codogno, E. Ogier-Denis, Celecoxib induces apoptosis by inhibiting 3-phosphoinositide-dependent protein kinase-1 activity in the human colon cancer HT-29 cell line, J. Biol. Chem. 277 (2002) 27613–27621.

[17] H.C. Lee, I.C. Park, M.J. Park, S. An, S.H. Woo, H.O. Jin, H.Y. Chung, S.J. Lee, H.S. Gwak, Y.J. Hong, D.H. Yoo, C.H. Rhee, S.I. Hong, Sulindac and its metabolites inhibit invasion of glioblastoma cells via down-regulation of Akt/PKB and MMP-2, J. Cell Biochem. 94 (2005) 597–610.

[18] E.M. Boon, J.J. Keller, T.A. Wormhoudt, F.M. Giardiello, G.J. Offerhaus, R. van der Neut, S.T. Pals, Sulindac targets nuclear β-catenin accumulation and Wnt signalling in adenomas of patients with familial adenomatous polyposis and in human colorectal cancer cell lines, Br. J. Cancer 90 (2004) 224–229.

[19] S. Dihlmann, A. Siermann, M. von Knebel Doeberitz, The nonsteroidal anti-inflammatory drugs aspirin and indomethacin attenuate β-catenin/TCF-4 signaling, Oncogene 20 (2001) 645–653.

[20] G. Hawcroft, M. D'Amico, C. Albanese, A.F. Markham, R.G. Pestell, M.A. Hull, Indomethacin induces differential expression of β-catenin, γ-catenin and T-cell factor target genes in human colorectal cancer cells, Carcinogenesis 23 (2002) 107–114.

[21] S. Dihlmann, S. Klein, M. von Knebel Doeberitz, Reduction of β-catenin/T-cell transcription factor signaling by aspirin and indomethacin is caused by an increased stabilization of phosphorylated β-catenin, Mol. Cancer Ther. 2 (2003) 509–516.

[22] S. Grösch, T.J. Maier, S. Schiffmann, G. Geisslinger, Cyclooxygenase-2 (COX-2)-independent anticarcinogenic effects of selective COX-2 inhibitors, J. Natl. Cancer Inst. 98 (2006) 736–747.

[23] A.H. Schönthal, Direct non-cyclooxygenase-2 targets of celecoxib and their potential relevance for cancer therapy, Br. J. Cancer 97 (2007) 1465–1468.

[24] N. Sakoguchi-Okada, F. Takahashi-Yanaga, K. Fukada, F. Shiraishi, Y. Taba, Y. Miwa, S. Morimoto, M. Iida, T. Sasaguri, Celecoxib inhibits the expression of survivin via the suppression of promoter activity in human colon cancer cells, Biochem. Pharmacol. 73 (2007) 1318–1329.

[25] M. Yamada, J. Ohnishi, B. Ohkawara, S. Iemura, K. Satoh, J. Hyodo-Miura, K. Kawachi, T. Natsume, H. Shibuya, NARF, an nemo-like kinase (NLK)-associated ring finger protein regulates the ubiquitylation and degradation of T cell factor/lymphoid enhancer factor (TCF/LEF), J. Biol. Chem. 281 (2006) 20749–20760.

[26] T.J. Maier, K. Schilling, R. Schmidt, G. Geisslinger, S. Grösch, Cyclooxygenase-2 (COX-2)-dependent and -independent anticarcinogenic effects of celecoxib in human colon carcinoma cells, Biochem. Pharmacol. 67 (2004) 1469–1478.

[27] S. Grösch, I. Tegeder, E. Niederberger, L. Bräutigam, G. Geisslinger, COX-2 independent induction of cell cycle arrest and apoptosis in colon cancer cells by the selective COX-2 inhibitor celecoxib, FASEB J. 15 (2001) 2742–2744.

[28] M. Ilyas, I.P. Tomlinson, A. Rowan, M. Pignatelli, W.F. Bodmer, B-catenin mutations in cell lines established from human colorectal cancers, Proc. Natl. Acad. Sci. USA 94 (1997) 10330–10334.

[29] I. Shureiqi, D. Chen, R. Lotan, P. Yang, R.A. Newman, S.M. Fischer, S.M. Lippman, 15-lipoxygenase-1 mediates nonsteroidal anti-inflammatory drug-induced apoptosis independently of cyclooxygenase-2 in colon cancer cells, Cancer Res. 60 (2000) 6846–6850.

[30] F. Takahashi-Yanaga, Y. Taba, Y. Miwa, Y. Kubohara, Y. Watanabe, M. Hirata, S. Morimoto, T. Sasaguri, Dictyostelium differentiation-inducing factor-3 activates glycogen synthase kinase-3β and degrades cyclin D1 in mammalian cells, J. Biol. Chem. 278 (2003) 9663–9670.

[31] K. Mayer, E. Wolff, H. Clevers, W.G. Ballhausen, The human high mobility group (HMG)-box transcription factor TCF-1:novel isoforms due to alternative splicing and usage of a new exon IXA, Biochim. Biophys. Acta 1263 (1995) 169–172.

[32] M. van de Wetering, J. Castrop, V. Korinek, H. Clevers, Extensive alternative splicing and dual promoter usage generate Tcf-1 protein isoforms with differential transcription control properties, Mol. Cell. Biol. 16 (1996) 745–752.

[33] M. van Noort, H. Clevers, TCF transcription factors, mediators of Wnt-signaling in development and cancer, Dev. Biol. 244 (2002) 1–8.

[34] L. Arce, N.N. Yokoyama, M.L. Waterman, Diversity of LEF/TCF action in development and disease, Oncogene 25 (2006) 7492–7504.

[35] A. Duval, S. Rolland, E. Tubacher, H. Bui, G. Thomas, R. Hamelin, The human T-cell transcriptional factor-4 gene: structure, extensive characterization of alternative splicings, and mutational analysis in colorectal cancer cell lines, Cancer Res. 60 (2000) 3872–3879.

Cardiovascular Research (2008) 77, 809–818
doi:10.1093/cvr/cvm095

# Aryl hydrocarbon receptor mediates laminar fluid shear stress-induced CYP1A1 activation and cell cycle arrest in vascular endothelial cells

**Zhiyi Han[1], Yoshikazu Miwa[1]*, Hiyo Obikane[2], Masako Mitsumata[2], Fumi Takahashi-Yanaga[1], Sachio Morimoto[1], and Toshiyuki Sasaguri[1]**

[1]*Department of Clinical Pharmacology, Faculty of Medical Sciences, Kyushu University, 3-1-1 Maidashi, Higashi-ku, Fukuoka 812-8582, Japan; and* [2]*Department of Pathology, Nihon University School of Medicine, Tokyo, Japan*

Received 10 April 2007; revised 19 November 2007; accepted 30 November 2007; online publish-ahead-of-print 7 December 2007

**Time for primary review: 29 days**

**KEYWORDS**
Aryl hydrocarbon receptor;
CYP1A1;
Shear stress;
Cell cycle;
Endothelial cell

**Aims** We investigated the mechanisms of shear stress (SS)-induced activation of cytochrome P450 (CYP) 1A1 and cell cycle arrest with regard to the role of the aryl hydrocarbon receptor (AhR), since AhR mediates the expression of CYP1A1 induced by polycyclic aromatic hydrocarbons (PAHs) and is thought to be involved in the regulation of cell growth and differentiation.

**Methods and results** Human umbilical vein endothelial cells (ECs) were exposed to laminar SS and thereafter collected to evaluate the expression, activity, and transcription of CYP1A1 and the expression of AhR and cell cycle-related proteins. A physiological level of laminar SS (15 dynes/cm$^2$) markedly increased the expression level and enzymatic activity of CYP1A1. SS stimulated CYP1A1 promoter activity without influencing mRNA stability. Loss of two functional xenobiotic response elements (XREs) in the 5′-flanking region of the CYP1A1 gene suppressed the SS-induced transcription of CYP1A1. Laminar SS stimulated the expression and nuclear translocation of AhR. α-Naphthoflavone, an AhR antagonist, and a small interfering RNA (siRNA) for AhR significantly suppressed SS-induced CYP1A1 expression. The siRNA also abolished SS-induced cell cycle arrest, the expression of the cyclin-dependent kinase inhibitor p21$^{Cip1}$, and dephosphorylation of retinoblastoma protein.

**Conclusion** Laminar SS stimulated the transcription of CYP1A1 through the activation of AhR in a way that is similar to the effects of PAHs. AhR was also involved in cell cycle arrest induced by SS. Our results suggest that sustained activation of AhR exposed to blood flow plays an important role in the regulation of EC functions.

## 1. Introduction

Aryl hydrocarbon receptor (AhR), a ligand-activated transcription factor, plays a central role in the induction of cytochrome P450 (CYP), especially CYP1A1, an enzyme produced on exposure to polycyclic aromatic hydrocarbons (PAHs) such as benzo(a)pyrene and 2,3,7,8-tetrachlorodibenzo-*p*-dioxin (TCDD).[1,2] On binding to AhR, PAHs translocate the receptor from the cytoplasm into the nucleus, where it forms a heterodimer with AhR nuclear translocator protein (ARNT). The dimer binds to the xenobiotic response elements (XREs) in the promoter region of the CYP1A1 gene to activate CYP1A1 transcription.[3] CYP1A1 generates harmful bioactive substances by metabolizing PAHs, and therefore, it is believed that AhR activation and subsequent CYP1A1 induction are aetiological factors for diseases such as cancers and atherosclerosis.[4]

In contrast, AhR is reported to contribute to normal physiological processes during cell growth and differentiation.[5] AhR-knockout mice exhibit a number of phenotypic abnormalities such as peripheral immune system deficiency, liver defects, and hypertrophic and fibrotic changes of the cardiovascular system, although the mice are resistant to TCDD toxicity.[6] In cultured cells, several studies suggest that the activation of AhR is involved in cell cycle arrest in the absence or presence of exogenous agonists.[7–9] These observations suggest that AhR may have important roles in physiological functions.

CYP1A1 is constitutively expressed in vascular endothelium *in vivo*[10]; however, the involvement of AhR has not been fully investigated. Vascular endothelial cells (ECs) are constantly exposed to haemodynamic forces, such as fluid shear stress (SS). Laminar SS plays an essential

* Corresponding author. Tel: +81 92 642 6082; fax: +81 92 642 6084.
*E-mail address*: ymiwa@clipharm.med.kyushu-u.ac.jp

role in the maintenance of the structure and function of blood vessels by regulating the expression of numerous genes and proteins.[11] Recent studies show that laminar SS strongly induces the expression of CYP1A1 in vascular ECs.[12,13] However, in spite of this, evidence suggests that laminar blood flow is atheroprotective.[14,15] Atherosclerosis tends to occur in areas exposed to disturbed flow or low SS, and a lack of SS induces apoptosis in ECs.[16] Therefore, we believe that the SS-induced sustained expression of CYP1A1 may have an important physiological role, in contrast to the transient induction by PAHs. In fact, loss of CYP1A1 is reported to correlate with dedifferentiation of cultured rat aortic ECs.[17]

Thus, in the present study, we examined the mechanism of expression of CYP1A1 induced by laminar SS in relation to the involvement of AhR in vascular ECs. Since we have reported that SS inhibits EC proliferation by inducing the expression of the cyclin-dependent kinase inhibitor $p21^{Cip1}$,[18] we also investigated the relationship between AhR and SS-induced cell cycle inhibition.

## 2. Methods

### 2.1 Chemicals

Actinomycin D (Act D), alpha-naphthoflavone (α-NF), and SB203580 were purchased from Sigma. U0126 was purchased from Cell Signaling Technology. SP600125 was purchased from LC Laboratories.

### 2.2 Cell culture

Human umbilical vein ECs (HUVECs) were isolated by collagenase digestion and cultured as described previously.[19] Human umbilical cords were obtained from healthy women who underwent uncomplicated term pregnancies. This investigation conforms to the principles outlined in the Declaration of Helsinki. Informed consent was obtained from each donor. Bovine arterial ECs (BAECs) were grown in Dulbecco's modified Eagle's medium containing 10% (v/v) foetal bovine serum (Hyclone), 100 U/mL penicillin, 100 mg/mL streptomycin, and 1 mg/mL amphoteracin B. Cells were used for experiments between passages 2 and 10.

### 2.3 Shear stress experiments

The laminar flow experiments were performed using a parallel plate chamber as described previously.[18] Briefly, cells were grown on gelatin-coated polyester sheets (Plastic Suppliers) until confluent. Control cells (static cells) were grown on the same polyester sheets in the same medium as sheared cells until confluent, and were transferred into fresh medium before being maintained in an incubator. A confluent monolayer of ECs on a polyester sheet was placed in a parallel-plate flow chamber and subjected to steady laminar shear stress. The flow loop with reservoirs and the flow chamber were filled with DMEM containing 10% foetal bovine serum.

To compare the effects of laminar and turbulent SS on the expression of CYP1A1 and AhR, a cone-plate type apparatus was used as previously described.[20] Cells were grown on a 10 cm dish until confluent and then exposed to laminar or turbulent SS using 0.5° or 5° cones, respectively, with a rotational velocity of 120 r.p.m. From the calculated modified Reynolds number ($R'$), turbulent flow was established at radii ≥2.4 cm, which corresponded to an $R' > 5$ and represented an average SS strength of 1.5 dyne/cm$^2$. Laminar SS strength was 6 dyne/cm$^2$. Cells were harvested from only the outer portion of the glass plate (≥2.4 cm).

### 2.4 Western blot analysis

Western blotting was performed as described previously,[21] using a polyclonal anti-CYP1A1 antibody (Santa Cruz Biotechnology), polyclonal anti-AhR antibody (Santa Cruz Biotechnology), polyclonal anti-ERK/phospho-ERK antibody (Cell Signaling Technology), monoclonal anti-JNK antibody and polyclonal anti-phospho-JNK antibody (Cell Signaling Technology), polyclonal anti-p38 mitogen-activated protein kinase (MAPK)/phospho-p38 MAPK antibody (Santa Cruz Biotechnology), polyclonal anti-$p21^{Cip1}$ antibody (Santa Cruz), and monoclonal anti-pRb antibody (Pharmingen). Nucleic and cytoplasmic proteins were purified using a Nuclear and Cytoplasmic Extraction Reagents kit (PIERCE), following the manufacturer's instructions. Membranes were re-probed with anti-β-actin monoclonal antibody to normalize the amounts of proteins applied to the SDS–PAGE gel, (Calbiochem).

### 2.5 Reverse transcription–polymerase chain reaction

Total cellular RNA was extracted with TRIzol Reagent (Invitrogen). The expression of mRNA was analysed by reverse transcription–polymerase chain reaction (RT–PCR) using Ready-To-Go RT–PCR Beads (Amersham Biosciences). The primers for human CYP1A1 and GAPDH were synthesized based on information obtained from the GenBank database: CYP1A1, 5′-GGATCTTTCTCTGTACCCTGG-3′ and 5′-AGCATGTCCTTCAGCCCAGA-3′; GAPDH, 5′-TCCACCACCCTGTTG CTGTA-3′ and 5′-ACCACAGTCCATGCCATCAC-3′; bovine CYP1A1, 5′-TCGGGCACATGCTGATGTTG-3′ and 5′-GCACAGATGACATTGGCC ACTG-3′; and bovine GAPDH 5′-AAGGCAGAGAACGGGAAGCT-3′ and 5′-TCCCTCCACGATGCCAAAGT-3′.

### 2.6 Measurement of CYP1A1 activity

CYP1A1 activity was evaluated with the ethoxyresorufin-*O*-dealkylase (EROD) assay, which measures the ability to convert ethoxyresorufin to resorufin, as described previously.[22]

### 2.7 Construction of plasmids and mutagenesis

The 5′-flanking region of rat CYP1A1 gene (−1166/+18) was amplified by PCR with 5′-GGTGAGATCTGCGCCCTTGCAAAGCTTAAGACTA-3′ as a sense primer and 5′-GGAGGAGCTTGGCACCACCACCTTTATATG-3′ as an antisense primer, and subcloned into the SacI/XhoI sites of a PGL3-basic luciferase-expressing reporter vector (Promega), a firefly luciferase reporter vector. For the two deletion constructs (DM-1 and DM-2), two restriction enzyme-digested fragments (DM-1, SacI/Bst1107I −859/+18; DM-2, SacI/BstEII −206/+18) were blunted and ligated using a DNA Blunting Kit (Takara). Site-directed mutagenesis was performed using QuickChange Site-directed Mutagenesis Kit (Stratagene), as instructed by the manufacturer. The luciferase reporter construct containing the −1166/+18 region of the CYP1A1 promoter was used as a DNA template. The mutations introduced into the putative binding sites for XRE were as follows: Mut-1 (−1069/−1052) CCCCCAGCTAGCGTGA CA→CCCCCAGCTAGTTAGACA; Mut-2 (−987/−970), TCTCACG CAACTCCGGGG→TCTCTAACAACTCCGGGG. Mut-3 has both mutations. The structure of every DNA construct was verified by sequencing.

siRNA duplexes were prepared by SAMCHULLY and targeted the coding regions of bovine AhR mRNA (770–778). The siRNA duplexes used in this study were as follows: siRNA for AhR (si-AhR), 5′-UACUUCCACCUCAGUUGGCTT-3′ and 5′-GCCAACUGAGGUGGAA GUATT-3′; Scramble (si-Scr), 5′-GCGCGCUUUGUAGGAUUCGTT-3′ and 5′-CGAAUCCUACAAAGCGCGCTT-3′, respectively.

### 2.8 Transfection and luciferase reporter assay

Transfection and luciferase reporter assays were performed as described.[23] Since we failed to amplify the fragment of human

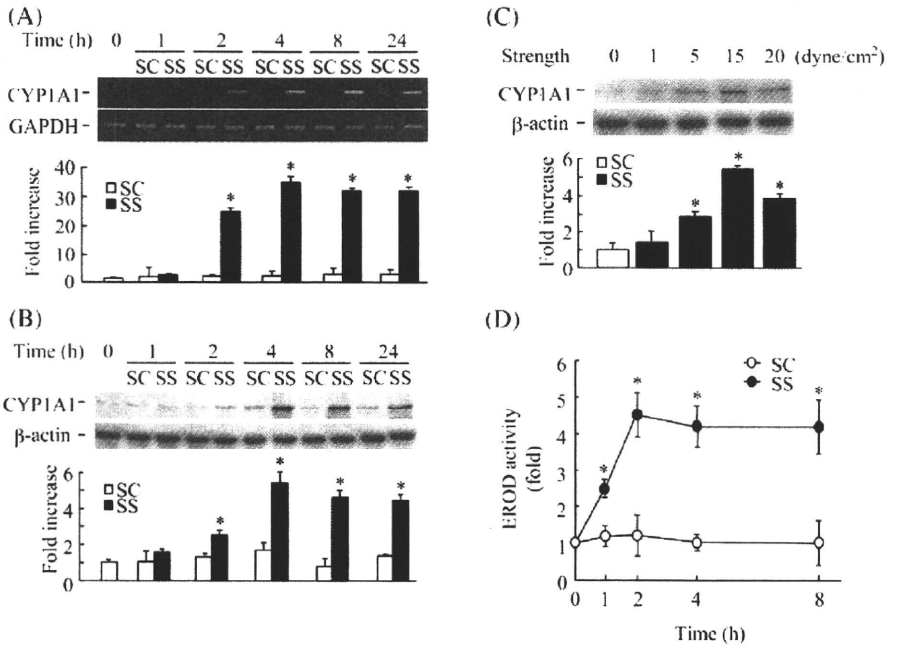


**Figure 1** Effects of shear stress (SS) on the expression and activity of CYP1A1 in endothelial cells. Human umbilical vein endothelial cells (HUVECs) were maintained in static conditions (SC) or exposed to laminar SS (SS, 15 dyne/cm$^2$) for the periods indicated (*A and B*). (*A*) CYP1A1 mRNA expression was analysed by reverse transcription–polymerase chain reaction (RT–PCR). (*B*) The time-course of CYP1A1 protein expressions induced by SS. (*C*) Strength dependency of CYP1A1 induction by laminar SS. HUVECs were exposed to laminar SS for 4 h at the indicated strengths. (*D*) CYP1A1 enzymatic activity in HUVECs was analysed by EROD assay as described in 'Methods' and plotted as a percentage of the value obtained in cells cultured under SC at time 0. Error bars represent the SD values obtained from four independent experiments. *$P < 0.01$ vs. SC. (*E*) HUVECs were exposed to SS for 4 h and thereafter treated with actinomycin D (Act D, 3 μmol/L), and incubated in static conditions (SC + Act D), or exposed to SS (SS + Act D). Expression levels of CYP1A1 mRNA normalized to those of GAPDH mRNA were standardized to the values obtained at the start time (−4 h), and the time-course after the administration of Act D is plotted in the lower panel. Error bars represent the SD values obtained from four independent experiments. (*F*) HUVECs (upper panel) or bovine arterial endothelial cells (BAECs) (lower panel) transfected with the plasmid containing the −1116/+18 region of the rat CYP1A1 promoter together with pRL-SV40 were incubated in SC, or exposed to laminar SS for 8 h. Mean raw values of firefly (CYP1A1) or renilla (control) luciferase activity are indicated below the panel. Relative luciferase activity is presented as the fold increase against the value obtained under SC. Data represent means ± SD of four independent experiments. *$P < 0.01$. (*G*) BAECs were maintained in SC or exposed to laminar SS (SS, 15 dyne/cm$^2$) for the periods indicated. *Upper panel*: CYP1A1 mRNA expression was analysed by RT–PCR. *Lower panel*: CYP1A1 protein expression was analysed by western blotting. Error bars represent the SD values obtained from four independent experiments. *$P < 0.01$ vs. SC. (*H*) CYP1A1 enzymatic activity in BAECs maintained in SC or exposed to laminar SS (SS, 15 dyne/cm$^2$) was analysed and plotted as described in *D*. *$P < 0.01$ vs. SC.

CYP1A1 promoter, we used rat CYP1A1 promoter in these assays because it has a high homology with the human CYP1A1 promoter. This is especially true of the four XRE motifs which show 93.3% (the first XRE), 92.9% (the second XRE), 93.1% (the third XRE), and 93.9% (the fourth XRE) homology. Excepting *Figure 1F*, promoter constructs were transfected into BAECs, because the efficiency of the transfection was much higher in BAECs (~70%) than in HUVECs (~20%). Cells were transiently transfected with plasmid DNA using LipofectAMINE regent (Life Technologies) as per the manufacturer's instructions. Simultaneously, pRL-simian virus 40 (pRL-SV40), which contained a Renilla luciferase gene with an SV40 promoter, was co-transfected as a control for transfection efficacy. Luciferase activity was measured using a double luciferase assay system (Toyo Ink Manufacturing Co.) and a Lumat LB9507 luminometer (Berthold Technologies). Firefly luciferase activity was normalized to Renilla luciferase activity to determine relative luciferase activity.

## 2.9 Fluorescence microscopy

After stimulation, the cells were fixed in ice-cold methanol/acetone (1:1) for 15 min at −20°C and then washed twice with phosphate-buffered saline. After blocking with 2% bovine serum albumin in phosphate-buffered saline for 30 min, cells were incubated overnight with polyclonal anti-AhR antibody (Santa Cruz Biotechnology, 1:200) at 4°C. Thereafter, cells were washed twice with phosphate-buffered saline and incubated with anti-rabbit IgG + IgA + IgM-biotin (Nichirei) for 1 h at room temperature, followed by streptavidin-fluorescein isothiocyanate conjugate (1:50 dilution; Invitrogen) for 1 h at room temperature. The cells were examined under a fluorescence microscope (Olympus).

## 2.10 Cell proliferation assay

To assess EC proliferation, we used the BrdU Cell Proliferation Assay (Exalpha Biologicals, Inc., MA, USA) according to the manufacturer's protocol. After stimulation, ECs were incubated overnight in culture medium containing BrdU (2 μl/ml). The uptake of BrdU was determined with a spectrophotometer (Bio-Tek Instruments, Highland Park, VT, USA) and normalized to the amount of cellular protein, which was measured in parallel samples according to the method of Lowry.

## 2.11 Statistics

Results are expressed as the mean ± SD of a number of the observations. Statistical significance was assessed by Student's *t*-test for paired or unpaired values.

# 3. Results

## 3.1 The induction and activation of CYP1A1 in response to shear stress

We first confirmed the effect of SS on the expression of CYP1A1 using HUVECs. Although the level of CYP1A1 mRNA

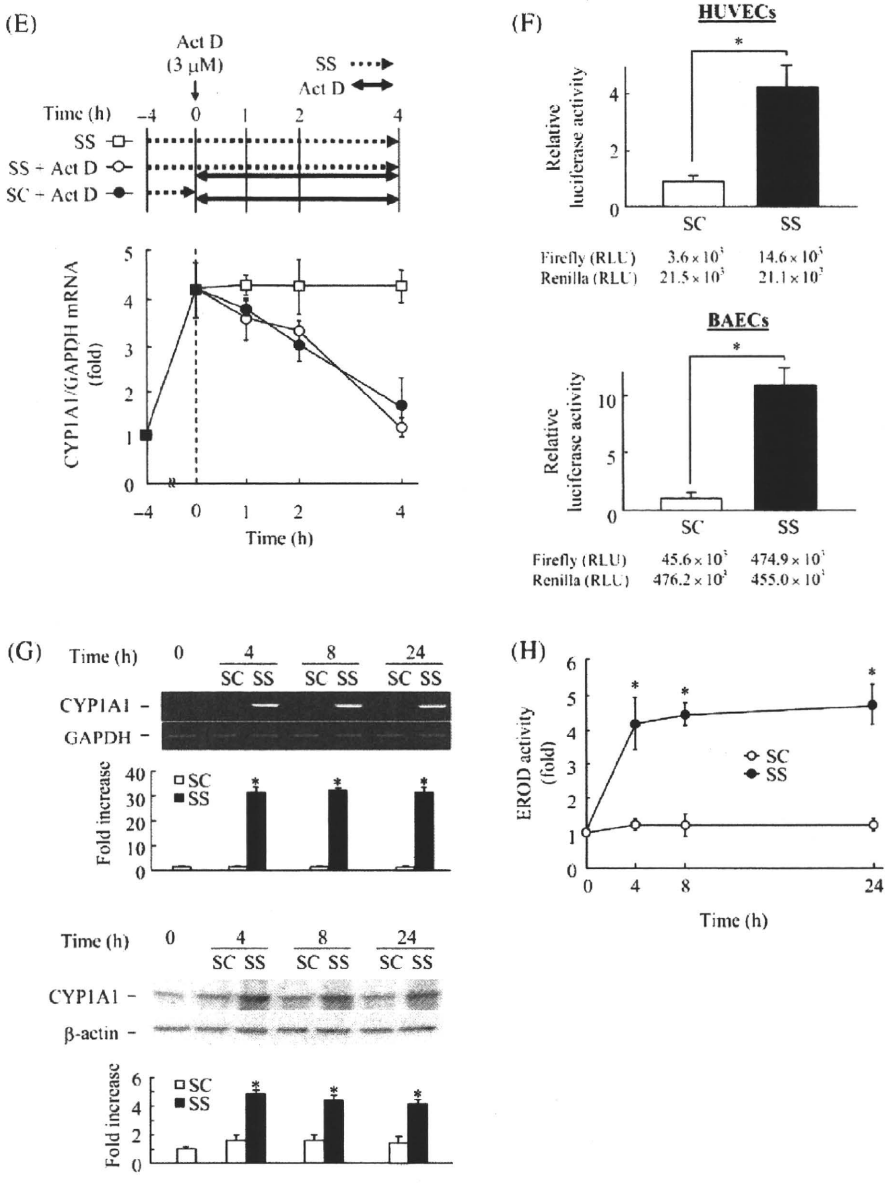


**Figure 1** Continued.

was very low in static control cells, it rose markedly on exposure to a physiological level of laminar SS (15 dyne/cm$^2$) (*Figure 1A*), consistent with previous reports.[12,13] The expression of CYP1A1 protein was also increased by SS and sustained over 24 h (*Figure 1B*). This CYP1A1 induction was SS strength-dependent (*Figure 1C*) and the expression level reached a maximal at 15 dyne/cm$^2$. As shown in *Figure 1D*, CYP1A1 activity determined by EROD assay was also increased by SS and reached a plateau after 2 h.

To investigate the mechanism of SS-induced CYP1A1 expression, we measured the rate of decay of the CYP1A1 mRNA after the addition of actinomycin D (Act D, 3 μmol/L), a transcription inhibitor. The degradation rates did not differ between the cells exposed to SS and those cultured in static conditions (*Figure 1E*). We also examined the effect of SS on CYP1A1 gene transcription in HUVECs transfected with a luciferase reporter construct driven by the 5′-flanking region of the rat CYP1A1 gene (−1116/+18 bp). Although the obtained raw values of luciferase activity were relatively low, it was significantly enhanced in HUVECs after exposure to SS for 8 h (*Figure 1F*, upper panel). When we did the same experiment using BAECs, the values of luciferase activity were much higher than those in HUVECs and furthermore, relative luciferase activity was strongly enhanced by SS (10.9-fold) (*Figure 1F*, lower panel). In BAECs, laminar SS induced mRNA and protein expressions (*Figure 1G*) and increased enzymatic activity of CYP1A1 (*Figure 1H*) as well as in HUVECs. These results suggest that SS induces CYP1A1 expression by activating gene transcription. The following transfection experiments were done using BAECs because of their higher transfection efficiency.